Dominant negative *SERPING1* variants cause intracellular retention of C1-inhibitor in hereditary angioedema
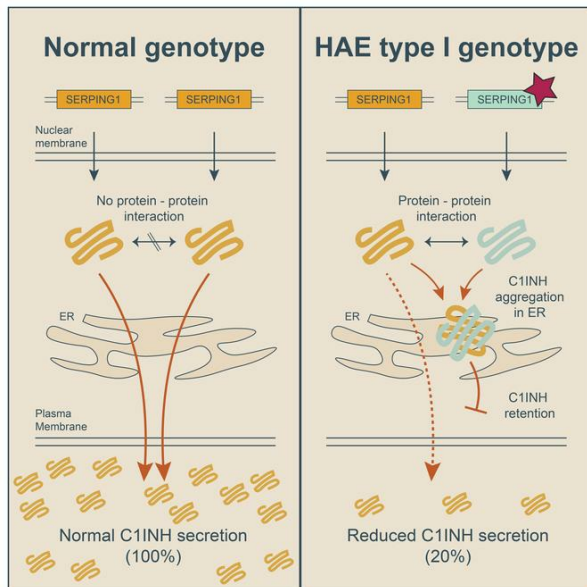
Didde Haslund, … , Lene N. Nejsum, Jacob Giehm Mikkelsen

Research In-Press Preview Cell biology Genetics

Graphical abstract

1   **Dominant negative *SERPING1* variants cause intracellular retention of C1-inhibitor**

2   **in hereditary angioedema**

3

4   Didde Haslund[1], Laura Barrett Ryø[1], Sara Seidelin Majidi[1], Iben Kløvgaard Rose[2],

5   Kristian Alsbjerg Skipper[1], Tue Fryland[1,3], Anja Bille Bohn[1], Claus Koch[4], Martin K.

6   Thomsen[1,5], Yaseelan Palarasah[4,6], Thomas J. Corydon[1,7], Anette Bygum[2], Lene N.

7   Nejsum[5] and Jacob Giehm Mikkelsen[1]

8

9   [1] Department of Biomedicine, Aarhus University, Aarhus C, Denmark

10   [2] Department of Dermatology and Allergy Centre, Odense University Hospital, Odense

11   C, Denmark

12   [3] iPSYCH, the Lundbeck Foundation Initiative for Integrative Psychiatric Research,

13   Denmark

14   [4] Department of Cancer & Inflammation Research, University of Southern Denmark,

15   Odense, Denmark

16   [5] Department of Clinical Medicine, Aarhus University, Aarhus, Denmark

17   [6] Unit for Thrombosis Research, Department of Regional Health Research, University of

18   Southern Denmark and Department of Clinical Biochemistry, Hospital of South West

19   Jutland, Esbjerg, Denmark

20   [7] Department of Ophthalmology, Aarhus University Hospital, Aarhus, Denmark

21

22

23   Corresponding author: Jacob Giehm Mikkelsen, Department of Biomedicine, Aarhus

24   University, Wilh. Meyers Allé 4, DK-8000 Aarhu C, Denmark. Phone: +4587167767.

25   Email: giehm@biomed.au.dk

1   **Abstract**

2

3   Hereditary angioedema (HAE) is an autosomal dominant disease characterized by

4   recurrent edema attacks associated with morbidity and mortality. HAE results from

5   variations in the *SERPING1* gene encoding C1 inhibitor (C1INH), a serine protease

6   inhibitor (serpin). Reduced plasma levels of C1INH lead to enhanced activation of the

7   contact system triggering high levels of bradykinin and increased vascular permeability,

8   but the cellular mechanisms leading to low C1INH levels (20-30% of normal) in

9   heterozygous HAE type I patients remain obscure. Here, we showed that C1INH encoded

10   by a subset of HAE-causing *SERPING1* alleles affected secretion of normal C1INH

11   protein in a dominant negative fashion by triggering formation of protein-protein

12   interactions between normal and mutant C1INH leading to creation of larger intracellular

13   C1INH aggregates that were trapped in the endoplasmic reticulum (ER). Notably,

14   intracellular aggregation of C1INH and ER abnormality were observed in fibroblasts

15   from a heterozygous carrier of a dominant negative *SERPING1* gene variant, but the

16   condition was ameliorated by viral delivery of the *SERPING1* gene. Collectively, our data

17   link abnormal accumulation of serpins, a hallmark of serpinopathies, with dominant

18   negative disease mechanisms affecting C1INH plasma levels in HAE type I patients and

19   may pave the way for new treatments of HAE.

Introduction

Hereditary Angioedema (HAE) is a rare autosomal dominant genetic disease with an estimated prevalence of 1:50,000 to 1:70,000 worldwide (1-3). HAE is characterized by recurrent non-pitting edema attacks of the deep dermis, submucosa, and subcutaneous tissues. Attacks often involve the extremities, the face, the gastrointestinal tract, and less frequently, but potentially life-threatening, the larynx (4). If not fatal, these very painful attacks are self-limiting and last up to five days.

HAE is caused by variants of the Serpin Family G member 1 (*SERPING1*) gene encoding the serine protease inhibitor (serpin) C1-inhibitor (C1INH) (5). To date, more than 450 different HAE-causing *SERPING1* gene variants, leading to either low levels (in case of HAE type I) or reduced function (in case of HAE type II) of C1INH (2, 6). HAE with normal C1INH level (HAE-nC1INH), in contrast, is reported to be caused by mutations in genes encoding other proteins encoding Factor XII (7), plasminogen (8), and angiopoietin 1 (9).

C1INH belongs to the largest and most diverse superfamily of protease inhibitors, the serpin superfamily (10), which also includes α1-antitrypsin (A1AT) and antithrombin. Serpins play a critical role in the control of proteases involved in blood coagulation as well as in inflammatory, complement and fibrinolytic pathways (11, 12), and their importance as crucial regulators of protease activity is emphasized by the number and severity of diseases caused by serpin dysfunction. Serpins share a highly conserved tertiary core structure (Figure 1A) comprised of three β-sheets (sA, sB and sC), eight or nine α-helices (termed hA-hI), and a protruding reactive center loop (RCL) (13). In native serpins, the RCL, located outside the tertiary core of the serpin, forms a flexible stretch of approximately 20 amino acids, which provides structural flexibility in a solvent-

exposed environment (14). The amino acid sequence of the RCL is numbered P17 (N-terminal) to P3′ (C-terminal). The peptide bond between P1 and P1′, referred to as the scissile bond, mimics the natural substrate and, thus, serves as a bait region for binding and cleavage of the targeted protease (15, 16). The protruding structure of the RCL makes it more accessible for interaction with target proteases, but it also causes the native serpin to be in a metastable form. When a target protease recognizes and cleaves the scissile bond, the RCL domain inserts into the central sA β-sheet as an additional strand and drags the covalently bound protease to the base of the serpin molecule (17, 18). After this dramatic conformational change, the serpin adopts a highly stable conformation, leading to irreversible inhibition of the protease (17).

Metastability of native serpins is a driving force for their inhibitory 'mouse-trap' function, but also renders serpins prone to polymerization (11). This tendency to form polymers can be further induced by mutations affecting the serpin structure and function, leading potentially to dysfunction and diseases collectively referred to as serpinopathies (10, 13). Formation of serpin polymers are known to cause disease in patients suffering from α1-antitrypsin deficiency (A1ATD) (19) and familial encephalopathy with neuroserpin inclusion bodies (FENIB) (20). According to the 'loop-sheet A' model, the most widely accepted model of polymer formation among serpins, long-chain serpin polymers are formed due to the capacity of the RCL of one serpin to dock into the sA of another serpin (21). Polymers of this type consisting of A1AT Z-variant subunits (Glu342Lys) (21) accumulate in the rough endoplasmic reticulum (ER) of hepatocytes and cause cell death and liver cirrhosis in patients suffering from A1ATD (22). Most serpinopathy-causing serpin defects are, like the in the A1AT Z-variant, located in the breach and shutter domains (Figure 1A) involved in facilitating the initial insertion of the RCL into the sA and accepting the RCL during protease inhibition, respectively. Thus, it

is hypothesized that defects within the breach and shutter domains destabilize and open the sA, thereby allowing the RCL of other serpins to dock in to this domain (19). Notably, polymers of C1INH protein have been detected in plasma isolated from HAE type I patients (23), but it remains unclear whether C1INH polymer formation occurs intracellularly and to which extent polymers affect the pathogenesis of HAE.

C1INH has central regulatory functions in several pathways that are part of the complement system, the fibrinolytic system, and the contact system. Under normal physiological conditions, C1INH regulates the contact system by inhibiting the activity of the two serine proteases FXIIa and kallikrein (24). However, the very low C1INH plasma level in HAE type I patients results in a poorly regulated contact pathway. It is widely accepted that enhanced activation of the contact system, leading to increased generation of the vasoactive peptide bradykinin, is a key trigger of the edema attacks observed in HAE patients (24, 25). Bradykinin formed in the contact system acts through the G-protein-coupled bradykinin B2 receptor on the surface of endothelial cells and causes increased vascular permeability and vasodilatation resulting in edema formation (5). C1INH is produced mainly in hepatocytes, reaching in healthy individuals a plasma concentration of 0.21-0.39 g/L (26). Of note, C1INH can be produced and secreted from other cell types like peripheral blood monocytes, fibroblasts and endothelial cells (27).

The majority of HAE patients are heterozygous carriers of a mutated *SERPING1* allele, resulting in production of functional C1INH only from a single allele. However, in most HAE type I patients the C1INH plasma level is reduced markedly below the expected level, often to around 20% of normal (28). These findings may potentially reflect an inhibitory role of mutated C1INH protein on C1INH protein derived from the wildtype *SERPING1* allele, but mechanisms explaining such 'trans-inhibition' have not been described. It has been suggested that the defective allele inhibits the synthesis of

normal C1INH (29), but evidence of a dominant negative action of mutated C1INH protein in the pathology of HAE is still lacking.

In this report, we demonstrate reduced cellular secretion of mutated C1INH protein expressed from alleles identified in patients suffering from HAE type I. Our findings provide evidence, to our knowledge for the first time, that C1INH encoded from HAE-causing *SERPING1* alleles can act upon C1INH expressed from the wildtype *SERPING1* allele in a dominant negative fashion, triggering the formation of intracellular C1INH aggregates and a resulting drop in the secretion of functional C1INH. Notably, such phenotypes are evident in skin-derived fibroblasts from patients carrying the most severe dominant negative allele. Collectively, our data indicate that reduced levels of C1INH leading to HAE type I are in a subset of patients caused by abnormal C1INH protein aggregation induced by mutated C1INH. Importantly, in patient-derived fibroblasts, the secretion barrier can be overcome by administration of the wildtype *SERPING1* gene, suggesting that dominant negative disease mechanisms can be overcome by gene supplementation providing hope for future development of gene therapies for HAE.

1 **Results**

2

3 **Reduced C1INH plasma levels in HAE type I patients carrying *SERPING1* gene**

4 **variants encoding full-length or near full-length C1INH**

5 Most HAE type I patients are heterozygous for mutations in the *SERPING1* gene and

6 maintain production of functional C1INH only from a single wildtype *SERPING1* allele.

7 However, the reduced plasma C1INH level in patients diagnosed with HAE type I

8 suggests that the C1INH level in the blood of HAE patients is affected by mechanisms

9 contributing to development of the disease. This led us to hypothesize that dominant

10 negative effects of the disease allele are evident intracellularly and directly involved in

11 restricting C1INH secretion leading to HAE type I. To investigate if such mechanisms

12 contribute to reduced plasma C1INH levels in HAE type I patients, we initially

13 investigated a total of six HAE type I-causing *SERPING1* gene variants present in Danish

14 HAE patients. As we reasoned that disease alleles encoding full-length or near full-length

15 C1INH proteins were most likely to have a dominant negative effect, we excluded disease

16 alleles giving rise to mRNA degradation and variants with gross gene rearrangements

17 from our analysis, and gene variants, for which premature stop codons were not

18 introduced and the reading frame was not affected, were selected (c.550G>A,

19 c.551_685del, c.566C>A, c.838_846del, c.1417G>A, and c.1427C>T; Figure 1B and

20 Supplementary Table S1). The location of each of these amino acid substitutions and

21 deletions in the predicted three-dimensional structure of C1INH are indicated in Figure

22 1A. Among the six patients carrying each of these *SERPING1* gene variants, five showed

23 severely reduced levels of plasma C1INH ranging from 0.05 to 0.13 g/L, whereas the

24 remaining patient had a plasma concentration of 0.2 g/L (Figure 1B).

25

1   **Reduced secretion of mutated C1INH protein from transfected cells**

2   To investigate the functional properties of the selected panel of HAE type I-causing

3   *SERPING1* gene variants, we initially established a cellular model system based on

4   ectopic expression of normal and mutated C1INH variants. First, a panel of expression

5   vectors encoding the different *SERPING1* gene variants was constructed (referred to as

6   pSERPING1[Variant], by which the type of mutation is indicated within the brackets)

7   (Figure 2A). Since C1INH is primarily produced in and secreted from the liver, we carried

8   out expression experiments in HepG2 cells, a human hepatocarcinoma cell line. Initially,

9   HepG2 cells were individually transfected with the seven different C1INH expression

10   constructs (six mutated variants and the wildtype *SERPING1* control), and the amount of

11   C1INH secreted into the medium was measured by sandwich ELISA. Also, untransfected

12   cells or cells transfected with an empty vector were included as negative controls. The

13   concentration of C1INH was $1,600 \pm 240$ ng/mL in medium from cells transfected with

14   pSERPING1[WT], whereas secretion of C1INH from cells transfected with plasmid

15   expressing HAE-causing *SERPING1* gene variants was severely reduced resulting in

16   background levels for several of the variants (Figure 2B). To verify that the reduced

17   C1INH secretion from cells expressing HAE-causing *SERPING1* variants was due to

18   impaired C1INH secretion and not insufficient C1INH expression, we generated a new

19   set of vectors in which the different *SERPING1* gene variants were fused to a human

20   influenza hemagglutinin (HA) tag (pSERPING1[Variant]-HA) (Figure 2A), allowing

21   evaluation of both secreted and intracellular C1INH-HA levels by Western blotting. As

22   shown in Figure 2C (quantification in Supplementary Figure S1A), only cells transfected

23   with pSERPING1[WT]-HA were capable of secreting C1INH into the medium to a level

24   that was detectable. Notably, intracellular HA-tagged C1INH was detectable in all cell

25   samples transfected with HAE-causing *SERPING1* gene variants, demonstrating that the

1   HAE-causing variants were indeed expressed after transfection. Interestingly, for all

2   variants we noted that the levels of intracellular HA-tagged C1INH was increased, for

3   three of the variants two-fold or more, relative to the positive control (Figure 2C,

4   Supplementary Figure S1B), suggesting that reduced secretion of C1INH correlated with

5   increased intracellular accumulation of the protein.

6   To establish an experimental platform allowing us to distinguish normal from

7   mutated C1INH and further assess cellular C1INH processing pathways, we set out to

8   generate a new set of expression vectors, in which the different *SERPING1* gene variants

9   were fused to a sequence encoding fluorescent mCherry protein (Figure 2A). Ectopic

10   production of C1INH carrying a fluorescent mCherry tag enabled analyses of both the

11   intracellular level and the secretion of C1INH from the same cells by measuring the

12   fluorescence intensity in cells and medium, respectively. To certify that the mCherry tag

13   did not itself hinder C1INH secretion, we confirmed by ELISA that mCherry-tagged

14   normal C1INH was indeed robustly secreted from plasmid-transfected HepG2 cells,

15   reaching levels of 240 ± 6 ng/mL in the medium (Figure 2D). Clearly, the level of

16   detectable C1INH carrying the mCherry tag was lower than the level obtained with

17   untagged C1INH (Figure 2B), which may reflect reduced detection using the C1INH

18   antibody, reduced expression or stability of the protein, posttranslational events affecting

19   transport or secretion, or potentially a combination of these effects. As expected, we did

20   not detect any C1INH protein in medium from cells transfected with plasmid encoding

21   the HAE-causing *SERPING1* gene variants (Figure 2D).

22   We then transfected HepG2 cells with the different pSERPING1[Variant]-

23   mCherry vectors and determined secreted and intracellular levels of mCherry-tagged

24   C1INH by measuring the fluorescence intensity. Using this approach, the amount of

25   C1INH-mCherry secreted into the medium from cells transfected with the six HAE-

1   causing *SERPING1* gene variants was found to be markedly reduced compared to cells

2   transfected with pSERPING1[WT]-mCherry (Figure 2E) confirming our previous

3   findings. Importantly, for all six variants increased intracellular C1INH-mCherry levels,

4   relative to the control, were measured by flow cytometry (Figure 2F), indicating that the

5   low level of secretion of mutated C1INH correlated with increased intracellular

6   accumulation and, thus, did not reflect reduced expression of C1INH. We performed a

7   similar experiment in HeLa cells with a higher transfection efficacy and confirmed

8   reduced secretion and increased intracellular accumulation of disease-causing C1INH

9   variants also in these cells (Figure 2G and 2H). We noted that this specific phenotype in

10   HeLa cells was particularly severe for the c.551_685del variant.

11

12   **Defective C1INH variants induce impaired secretion and enhanced intracellular**

13   **accumulation of co-expressed normal C1INH**

14   To model the co-expression of two *SERPING1* alleles in HAE type I patients, we took

15   advantage of mCherry-tagged C1INH protein variants using the approach schematically

16   depicted in Figure 3A. To evaluate the effect of mutated C1INH on secretion and

17   intracellular accumulation as well as on localization of normal C1INH tagged with

18   mCherry, HepG2 and HeLa cells were transfected with equal amounts of

19   pSERPING1[WT]-mCherry and vectors encoding HAE-causing *SERPING1* gene

20   variants (pSERPING1[variant]). First, we found that secreted levels of normal C1INH-

21   mCherry were reduced in medium from cells simultaneously expressing one of the six

22   defective C1INH variants relative to cells co-transfected with pcDNA as a negative

23   control (Figure 3B). We also found that co-expression of normal C1INH-mCherry with

24   normal C1INH resulted in this assay in increased secretion of mCherry-tagged C1INH

25   protein. Next, in concordance with reduced secretion, we measured an increase in the

intracellular level of normal C1INH-mCherry in all cultures expressing the HAE-causing *SERPING1* gene variants compared to control cells (Figure 3C), supporting the notion that the examined defective C1INH variants interfered with secretion of co-expressed normal C1INH-mCherry and thus induced intracellular accumulation of mCherry-tagged normal C1INH. Once again, the c.551_685del variant was found to induce the most severe accumulation phenotype (Figure 3C). In HeLa cells, similar co-transfection experiments showed reduced secretion of normal C1INH-mCherry only in cells co-expressing C1INH from pSERPING1[c.551_685del] (Figure 3D), whereas increased intracellular levels of C1INH-mCherry were evident 72 hours after transfection for four of the six *SERPING1* expression constructs (c.550G>A; c.551_685del; 566C>A; c.838_846del) with c.551_685del and 566C>A *SERPING1* variants causing the highest levels of protein accumulation (Figure 3E). In summary, these findings suggest that HAE-causing *SERPING1* gene variants encode C1INH that restricts secretion of functional C1INH and thus induces cellular phenotypes in a dominant negative fashion.

To evaluate the strength of mutated C1INH as a dominant negative inhibitor, we carried out a dose-response experiment with the c.551_685del variant, which seemed to show the most profound phenotype. By co-transfection of HeLa cells with pSERPING1[WT]-mCherry (450 ng) and increasing amounts of pSERPING1[c.551_685del] (50, 200, 450, 700, or 900 ng), a gradual decrease of normal C1INH-mCherry secretion with increasing amounts of plasmid encoding defective C1INH was observed (Figure 3F). In accordance, flow cytometry analysis of transfected cells showed gradually increased levels of intracellular C1INH-mCherry (Figure 3G), indicating that cellular transport and secretion of C1INH-mCherry was massively blocked by defective C1INH protein. In contrast, in control samples co-transfected with pSERPING1[WT], C1INH-mCherry secretion was enhanced with increasing amounts of

1 plasmid, whereas intracellular levels were unaffected (Figure 3F and 3G). In summary,

2 our data suggest that C1INH variants expressed in HAE patients act as dominant negative

3 inhibitors inducing intracellular accumulation and reduced secretion of functional

4 C1INH.

5

6 **Intracellular congestion of normal C1INH induced by HAE-causing C1INH**

7 **variants**

8 Using the model system based on mCherry-tagged C1INH, we moved on to investigate

9 the intracellular localization of C1INH by live widefield microscopy. Due to the small

10 size of HepG2 rendering these cells unsuitable for microscopy-based analysis, we

11 performed these analyses in HeLa cells. First, intracellular localization of the different

12 C1INH-mCherry variants was visualized in HeLa cells transfected with the different

13 pSERPING1[Variant]-mCherry vectors. As seen in Figure 4A, C1INH-mCherry derived

14 from pSERPING1[WT]-mCherry was evenly distributed throughout the entire cell almost

15 in a reticular pattern. Out of the six HAE-causing *SERPING1* gene variants, the cellular

16 C1INH-mCherry pattern was clearly altered only in cells transfected with

17 pSERPING1[c.566C>A]-mCherry (encoding C1INH$_{Thr167Asn}$-mCherry) relative to cells

18 transfected with pSERPING1[WT]-mCherry (Figure 4A). In these cells, we observed

19 accumulation of C1INH$_{Thr167Asn}$-mCherry in patterns reminiscent of localized aggregates,

20 correlating with the low levels of C1INH secretion and increased intracellular

21 accumulation observed previously for this variant (Figure 2G and 2H).

22 To investigate if the mutated C1INH variants in a dominant negative fashion

23 induced formation of intracellular aggregates containing co-expressed normal C1INH-

24 mCherry protein, HeLa cells were in a series of transfections co-transfected with

25 pSERPING1[WT]-mCherry and vectors encoding each of the HAE-causing *SERPING1*

gene variants (pSERPING1[Variant]). Notably, relative to the controls, marked changes in the intracellular distribution of normal C1INH-mCherry were evident in cells co-expressing the c.550G>A, c.551_685del, and c.566C>A *SERPING1* variants, respectively (Figure 4B). For all three variants, the emergence of a number of well-defined fluorescent foci unveiled a very distinct cellular phenotype, which was over several experiments reproducibly most severe in cells expressing C1INH$_{Gly162\_Pro206del}$ encoded by pSERPING1[c.551_685del]. As this phenotype correlated well with the reduced secretion and dominant negative effects of this variant, we intensified the analysis of this particular *SERPING1* allele.

Next, we addressed whether the formation of fluorescent foci could potentially be an artifact of overexpressing C1INH$_{Gly162\_Pro206del}$. To evaluate if there was a correlation between the formation of C1INH-mCherry aggregates and the amount of mutant protein, cells were co-transfected with a fixed amount of pSERPING1[WT]-mCherry and increasing amounts of pSERPING1[c.551_685del], or pSERPING1[WT] as a control. Even with increased amounts of pSERPING1[WT], we did not observe formation of C1INH-containing foci (Supplementary Figure S2A). In contrast, even with the lowest amount of pSERPING1[c.551_685del], fluorescent foci were firmly generated, and formation of foci did not seem to be further boosted with increasing dosages of transfected plasmid (Supplementary Figure S2B). Together, these findings showed that the formation and size of intracellular C1INH aggregates was not directly correlated to the amount of protein and that the abnormal cellular phenotype did not originate from massive overproduction of the inhibitory protein.

Prominent intracellular C1INH focus formation induced by C1INH$_{Gly162\_Pro206del}$ as quantified by Imagestream® analysis

To evaluate the prevalence of the cellular C1INH aggregation phenotype observed in cells co-expressing normal C1INH and C1INH$_{Gly162\_Pro206del}$, we set out to quantify formation of fluorescent foci using Imagestream® technology (30), allowing high-resolution microscopy and computational analysis of thousands of cells expressing C1INH-mCherry. HeLa cells were co-transfected with pSERPING1[WT]-mCherry and either pcDNA, pSERPING1[WT], or pSERPING1[c.551_685del]. Untransfected cells were included as a negative control. 20,000 cells from each co-transfection were analyzed (Figure 4C). The number of mCherry-positive cells in each group ranged between 1,395 and 3,579, with zero mCherry-positive cells in the negative control. The percentage of cells with accumulation of C1INH-mCherry protein in the cell perimeter was defined using the Max Contour Position feature describing the location of high intensity C1INH-mCherry protein. The position was represented by a number between 0 and 1, with 0 being the center of the cell and 1 being the perimeter of the cell. By visual inspection of the generated cell images, foci of normal C1INH-mCherry were prevalent in cells with a Max Contour Position above 0.5 (Condensed gate in Figure 4C, right panel). 11.4% and 12.3% of the mCherry-positive cells co-transfected with pSERPING1[WT]-mCherry and either pcDNA or pSERPING1[WT], respectively, had a Max Contour Position above 0.5. In contrast, 59.1% of the mCherry-positive cells co-transfected with pSERPING1[WT]-mCherry and pSERPING1[c.551_685del] had a Max Contour Position above 0.5 (Condensed gate, Figure 4C), emphasizing that the inclusion of normal C1INH in larger aggregate-like formations was induced when C1INH$_{Gly162\_Pro206del}$ was co-expressed in transfected cells.

Blockage of accumulated C1INH within the ER

It is widely accepted that aggregation of serpin polymers within the ER is part of the pathology of serpinopathies like α1-antitrypsin deficiency (20). To investigate if aggregates of normal C1INH induced by defective C1INH protein indeed accumulated within the ER, HeLa cells were co-transfected with equal amounts of pSERPING1[WT]-HA and pcDNA, pSERPING1[WT], or pSERPING1[c.551_685del] (Figure 5). To visualize ER in subsequent microscopy analyses, an expression plasmid encoding a Tomato fluorescence gene fused to an ER-targeting sequence was included in the transfections. By staining for HA-tagged normal C1INH, we observed a diffuse distribution pattern suggesting that normal C1INH co-localized with ER in cells co-transfected with pcDNA or pSERPING1[WT] (Figure 5, upper two rows). Aggregate-like structures containing normal C1INH-HA formed in the presence of pSERPING1[c.551_685del] and clearly accumulated within the ER (Figure 5, bottom row). Interestingly, in contrast to the reticular-like ER structure observed in cells co-transfected with pcDNA or pSERPING1[WT], the ER structure underwent dramatic alterations in cells co-transfected with pSERPING1[c.551_685del], showing a constipated ER structure adapting the shape of the C1INH-HA foci. Of note, using an alternative approach by which ER in HeLa cells was visualized with an antibody recognizing the KDEL motif, we observed the same phenomenon in cells co-transfected with pSERPING1[WT]-mCherry and pSERPING1[c.551_685del] (Supplementary Figure S3). Collectively, these findings suggested that C1INH$_{Gly162\_Pro206del}$ inhibits the secretion of C1INH in a dominant negative fashion by inducing accumulation of normal C1INH in the ER. As this phenotype showed pronounced similarity to cellular phenotypes suggested to cause α1-antitrypsin deficiency (A1ATD), our results prompted us to

1 validate and compare aggregation of the two serpins in our cellular model system based

2 on fusing serpins to mCherry.

3   In A1ATD caused by the frequent Z variant of the SERPINA1 gene, the plasma

4 level of α1-antitrypsin is significantly reduced in patients that are homozygous for the Z

5 variant compared to healthy individuals carrying two normal SERPINA1 alleles (referred

6 to as 'M' alleles) (19). To mimic this scenario, HeLa cells were transfected with vectors

7 encoding either an mCherry-tagged M or Z SERPINA1 cDNA variant

8 (pSERPINA1[Variant]-mCherry), and the secreted and intracellular levels of α1-

9 antitrypsin-mCherry were determined by quantification of fluorescence, as previously

10 described. As shown in Supplementary Figure S4A, the amount of secreted α1-antitrypsin

11 in HeLa cells transfected with pSERPINA1[Z]-mCherry was reduced to 50% of the

12 amount secreted from cells transfected with pSERPINA1[M]-mCherry. The reduction in

13 α1-antitrypsin secretion correlated with an increase in the intracellular level of α1-

14 antitrypsin in cells transfected with pSERPINA1[Z]-mCherry compared to cells

15 transfected with pSERPINA1[M]-mCherry (Supplementary Figure S4B). To evaluate if

16 reduced secretion and increased intracellular levels of the Z-variant in this setup was due

17 to accumulation of α1-antitrypsin in the ER, as previously demonstrated (19), transfected

18 HeLa cells were stained for the ER using an antibody recognizing KDEL (Supplementary

19 Figure S4C). Notably, in cells transfected with pSERPINA1[M]-mCherry, α1-

20 antitrypsin-mCherry co-localized with ER in a reticular-like structure. However, in

21 contrast, in cells transfected with pSERPINA1[Z]-mCherry, foci were formed and

22 retained in ER, exactly as we observed for accumulating C1INH, resulting in structural

23 changes of the ER.

24   In summary, these data consolidate the use of this cell model system for studies

25 of serpin localization and secretion. Our findings suggest that the cellular aggregation

1   phenotypes induced by the α1-antitrypsin Z-variant and C1INH$_{Gly162\_Pro206del}$ encoded by

2   SERPING1[c.551_685del] share important characteristics and lend support to the notion

3   that serpin aggregation affects C1INH secretion in patients with the c.551_685del

4   mutation similar to how the Z-mutation affects secretion of α1-antitrypsin in A1ATD

5   patients.

6

7   **Co-localization of normal and defective C1INH protein in focus-forming aggregates**

8   To determine if normal and defective C1INH protein co-localize within the formed

9   protein foci, HeLa cells were co-transfected with pSERPING1[WT]-mCherry and

10   pSERPING1[c.551_685del]-HA, producing differently tagged C1INH variants, which

11   allowed us to distinguish between normal and defective C1INH protein. Cells co-

12   transfected with pSERPING1[WT]-mCherry and pSERPING1[WT]-HA were included

13   as a control. As expected, C1INH foci were only formed in cells in which

14   pSERPING1[WT]-mCherry was co-transfected with pSERPING1[c.551_685del]-HA,

15   and normal C1INH-mCherry and C1INH$_{Gly162\_Pro206del}$-HA protein localized to the same

16   cellular structures (Figure 6A). In summary, these data support that physical co-

17   localization of mutant and normal C1INH contributes to aggregate formation and the

18   dominant-negative effects of defective C1INH protein.

19

20   **Normal C1INH and C1INH$_{Gly162\_Pro206del}$ are directly associated in C1INH polymers**

21   To investigate whether formation of aggregates consisting of normal C1INH and

22   C1INH$_{Gly162\_Pro206del}$ involved direct association between the two variants, we performed

23   co-immunoprecipitation (co-IP) assays using different sets of tagged variants. First,

24   untagged normal and C1INH$_{Gly162\_Pro206del}$ were separately expressed or co-expressed in

25   HeLa cells. Using a C1INH antibody detecting both C1INH protein variants, we first

1   verified by Western blotting that secretion of C1INH$_{Gly162\_Pro206del}$ was markedly reduced

2   relative to normal C1INH (Figure 6B, top panel, Supplementary Figure S5A). Notably,

3   as opposed to cells expressing normal C1INH, higher amounts of C1INH protein was

4   detected in the soluble and insoluble fractions of cellular protein derived from cells

5   expressing the disease variant. (Figure 6B, bottom panels, Supplementary Figure S5B-

6   S5C). These findings recapitulated that aggregated C1INH protein accumulated in cells

7   expressing C1INH$_{Gly162\_Pro206del}$. Next, we co-expressed HA-tagged normal C1INH with

8   C1INH$_{Gly162\_Pro206del}$ in HeLa cells and noted the inhibitory effect of C1INH$_{Gly162\_Pro206del}$

9   on secretion of HA-tagged C1INH relative to cells expressing normal C1INH-HA alone

10   (Figure 6C, top panel, Supplementary Figure S5D). Interestingly, only in the presence of

11   C1INH$_{Gly162\_Pro206del}$, HA-tagged normal C1INH also appeared in the insoluble fraction

12   of cellular protein, suggesting that normal protein was restrained in the insoluble fraction

13   by the mutated protein (Figure 6C, lower panels, Supplementary Figure S5E-S5F).

14   Finally, we transfected HeLa cells with plasmid encoding either V5-tagged normal

15   C1INH or HA-tagged C1INH$_{Gly162\_Pro206del}$, or co-transfected with a combination of these

16   variants, and performed co-IP on whole cell lysates by incubating with anti-V5-coupled

17   beads to capture V5-tagged protein and potential interacting proteins. It was verified first

18   that V5- and HA-tagged C1INH variants were equally present in the input (Figure 6D,

19   top panel, Supplementary Figure S5G-S5H). As the presence of C1INH-V5 was evident

20   in the captured fraction, we then blotted for the presence of HA-tagged C1INH protein

21   among captured complexes. Notably, HA-tagged C1INH$_{Gly162\_Pro206del}$ was detected when

22   the protein was expressed together with V5-tagged C1INH, whereas normal HA-tagged

23   protein was not captured in the presence of V5-tagged C1INH (Figure 6D, lower panel,

24   Supplementary Figure S5I-S5J). These findings demonstrate that direct protein-protein

25   interactions   are   formed   between   normal   C1INH   and   the   HAE-causing

C1INH_{Gly162_Pro206del} variant, whereas normal C1INH does not alone engage in such complex formation.

C1INH aggregates are prominent in patient fibroblasts carrying the c.551_685del *SERPING1* gene variant

To our knowledge, aggregates of C1INH protein have not previously been detected in cells derived from HAE type I patients. It was critical, therefore, to investigate whether aggregate formation was also evident in C1INH-expressing patient cells. As we did not have access to patient hepatocytes, we set out to study C1INH production and secretion in cultures of skin-derived fibroblasts, as was previously demonstrated by Kramer and colleagues (31). Fibroblasts were isolated and expanded from three HAE type I patients carrying the c.550G>A, c.551_685del, and c.838_846del *SERPING1* alleles, respectively. First, to confirm that patient-derived fibroblasts could be exploited as a cellular model of the disease, C1INH secretion from each of the cultures as well as from three fibroblast cultures derived from healthy donors was measured by sandwich ELISA. Notably, for all three patients, secretion of C1INH from fibroblasts was significantly reduced relative to the controls (Figure 7A). For two of the three patient samples (c.551_685del and c.838_846del), secretion was severely reduced, resulting in C1INH medium levels corresponding to 10-30% of the levels observed with the controls (Figure 7A). Among the six samples, some variation in the levels of *SERPING1* mRNA was observed. Despite a vague indication of lower mRNA levels in patient samples, comparable levels of *SERPING1* mRNA was measured in patient-derived cells relative to the control showing the lowest level of expression (NHDF-15) (Figure 7B), suggesting that differences in C1INH secretion did not reflect major differences in RNA production or processing. Notably, using fibroblasts derived from the patient carrying the

1   c.551_685del allele, we performed a PCR on cDNA with *SERPING1* primers spanning

2   the deletion and demonstrated by gel analysis that the normal allele and the allele carrying

3   the deletion were equally expressed in the patient cells (Figure 7B, insert).

4   To demonstrate the impact of the c.838_846del allele on the normal allele, we first

5   transduced primary fibroblasts (NHDF-03) from a homozygous healthy donor with

6   lentiviral vectors encoding c.551_685del at an estimated MOI of 1. Relative to

7   untransduced cells and cells treated with eGFP-encoding lentiviral vectors, secretion from

8   cells expressing the mutant protein was severely restricted resulting in levels that were

9   almost halved compared to the controls (Figure 7C). Collectively, these findings were

10   consistent with a model by which C1INH encoded by the disease allele induced reduced

11   secretion by dominant negative actions.

12   To investigate whether aggregate formation and structural ER changes were

13   evident in fibroblasts from the patient carrying the c.551_685del allele, we transfected

14   control and patient-derived fibroblasts with the expression plasmid encoding the Tomato

15   fluorescence gene fused to an ER-targeting sequence. In all three cultures of control

16   fibroblasts (derived from three different donors) a diffuse and reticular-like ER structure,

17   corresponding to the structure that was observed in HeLa cells expressing only normal

18   C1INH (Figure 5), was observed (Figure 7D). Importantly, in fibroblasts derived from

19   the patient we noted that the overall ER structure was significantly different (Figure 7D,

20   right panel) and very similar to the ER structure that we observed in HeLa cells co-

21   transfected with pSERPING1[WT]-mCherry and pSERPING1[c.551_685del] (Figure 5).

22   Next, we transfected control and patient-derived fibroblasts with plasmid

23   encoding the ER-targeted Tomato fluorescence protein and then stained the cells with a

24   monoclonal C1INH antibody recognizing both normal and defective C1INH protein. In

25   all control fibroblasts, C1INH co-localized with the reticular-like ER structure (Figure

7E), as seen earlier in the transfected control samples of HeLa cells. In patient cells, in contrast, the staining of C1INH revealed a distinct, speckled pattern that was significantly different from the pattern in control fibroblasts, demonstrating that C1INH and fluorescent ER-targeted protein localized to the same cellular structures (Figure 7E). We confirmed this cellular phenotype by staining fibroblasts that were co-transfected with pSERPING1[WT]-HA and plasmid encoding Tomato fluorescence gene fused to an ER-targeting sequence with an HA-specific antibody (Supplementary Figure S6). In conclusion, our data unveil aberrant accumulation of C1INH protein and the appearance of a distinct ER structural phenotype in cells from a HAE type I patient carrying a heterozygous in-frame deletion within the *SERPING1* gene.

Identification of other dominant-negative HAE-causing *SERPING1* variants

Aggregate formation caused by protein-protein interactions between normal and mutated C1INH explains a dominant-negative phenotype resulting in reduced secretion of functional C1INH. However, among the HAE-causing mutations that were initially selected for this study, the severity of aggregate formation varied and larger protein aggregation foci, formed in the presence of both normal and mutant protein, were seen only for two variants (c.551_685del and c.566C>A). Considering the wealth of different *SERPING1* variants causing HAE, we set out to identify other *SERPING1* alleles acting through similar mechanisms. Since the shutter domain of the protein is afflicted in C1INH derived from both c.551_685del and c.566C>A variant, we decided to focus on this region of the protein and identified the β-sheets and α-helices that are part of or in close proximity to the shutter domain. A total of ten HAE-causing *SERPING1* variants were selected from the 'C1 inhibitor gene mutation database' (32). Each of these ten gene variants encodes a full-length C1INH protein (478-aa) with a single amino acid change

within or near the shutter domain (Figure 8A; Supplementary Figure S7; Supplementary Table S2). First, by transfection of expression constructs (pSERPING1[Variant]) into HepG2 cells and subsequent Western blot analysis, we observed robust protein production and reduced secretion of C1INH for eight of the ten variants as measured 72 hours after transfection (Figure 8B, Supplementary Figure S8A-S8B). For three of these variants, c.508T>C, c.530T>C, and c.707T>C, secretion was entirely blocked. Next, to investigate the inhibitory impact of mutated C1INH on normal C1INH, we co-transfected the expression constructs with the pSERPING1[WT]-mCherry reporter construct and measured mCherry intensity in medium and in cells. For five of the variants, we found that secretion of the mCherry-tagged normal C1INH was inhibited by the mutant protein like the effect caused by the c.551_685del variant (Figure 8C). Also, for some of the variants we found that the intracellular levels of C1INH-mCherry were significantly increased although not with the same impact as reproducibly observed for the c.551_685del variant (Figure 8D). We demonstrated that these effects were evident already 48 hours after transfection (Supplementary Figure S9). Interestingly, by wide-field microscopy, we observed formation of foci containing normal mCherry-tagged C1INH in cells expressing the c.530T>C, c.707T>C, c.863_864TC>AA, and c.871A>C *SERPING1* variants (Figure 9A). Importantly, none of the ten C1INH variants showed any indication of forming protein aggregates, when they were expressed separately (and in the absence of normal C1INH) in HeLa cells (Supplementary Figure S10). However, normal C1INH-HA was prevalent in the insoluble protein fraction derived from cells in which normal C1INH-HA was co-expressed with C1INH from the c.508T>C, c.530T>C, c.707T>C, c.863_864TC>AA, and c.871A>C gene variants (Figure 9B, lower panel, quantifications in Supplementary Figure S11A-S11C). This mimicked the pattern that we also observed for c.551_685 del (included as control in Figure 9B). In contrast, for cells

co-transfected with pSERPING1[WT]-HA and pcDNA, normal C1INH-HA was detectable in the soluble protein fraction, but not in the insoluble fraction (Figure 9B, middle and lower panel).

Finally, for the three variants (c.530T>C, c.707T>C, and c.863_864TC>AA) showing both reduced secretion and dominant negative intracellular retention of normal C1INH as well as the capacity to induce aggregation of normal C1INH, we performed Co-IP to unveil protein-protein interactions between C1INH variants and normal C1INH. Again, HA-tagged disease variants were co-expressed with V5-tagged normal protein and capture of V5-tagged C1INH verified by Western blotting (Figure 9C, quantifications in Supplementary Figure S11D-S11G). Notably, by blotting among captured protein complexes using an HA-specific antibody, we detected considerable amounts of HA-tagged C1INH protein, demonstrating that all three disease-causing C1INH variants engaged in direct protein-protein interactions with normal C1INH (Figure 9C, lower panel). Collectively, these findings suggest that dominant negative phenotypes involving protein-protein association and aggregate formation are evident for several *SERPING1* variants causing HAE.

Amelioration of reduced C1INH secretion in HAE type I patient fibroblasts by delivery of a therapeutic *SERPING1* gene

The identification of a dominant negative disease mechanism leading to HAE type I may inspire new ways to restore C1INH secretion and treat HAE type I. Here, we focus on exploiting genetic strategies to overcome restriction on C1INH secretion caused by C1INH protein aggregation induced by the dominant negative effect of mutant C1INH protein. To study whether such inhibitory effects could be overcome by delivering a gene expression cassette coding for normal C1INH, we initially created HeLa cells carrying

1   expression cassettes encoding either normal C1INH or C1INH$_{Gly162\_Pro206del}$ (from

2   SERPING1[c.551_685del]). Next, we transduced these cell lines with lentiviral vectors

3   carrying the SERPING1[WT] cDNA expressed from the phosphoglycerate kinase (PGK)

4   promoter. Untransduced cells as well as cells transduced with eGFP-encoding lentiviral

5   vectors were included as controls. As expected, secretion of C1INH was dramatically

6   higher from untransduced cells expressing the wildtype *SERPING1* gene compared to

7   cells expressing C1INH$_{Gly162\_Pro206del}$ (Figure 10A). In addition, treatment of C1INH-

8   secreting HeLa cells with C1INH-encoding lentiviral vectors increased the level of

9   secreted C1INH from 1,000 to 4,500 ng/mL, whereas treatment with the viral vector

10   raised the level of secreted C1INH from cells expressing C1INH$_{Gly162\_Pro206del}$ from

11   background level to 2,500 ng/mL (Figure 10A). These findings indicated that the

12   restrictive effect of the mutant variant could be overcome by viral gene transfer. To test

13   this gene therapy delivery approach directly in patient cells, we delivered C1INH-

14   expressing lentiviral vectors and control vectors to control and patient fibroblasts. For all

15   control fibroblasts, we observed a marked increase in the secretion of C1INH, leading to

16   levels in the medium ranging from 7,000 to 12,000 ng/mL (Figure 10B). Also in these

17   cells, we observed a tendency to reduced C1INH secretion upon treatment with eGFP-

18   encoding lentiviral vectors (although not with statistical significance), potentially

19   indicating a toxic or inhibitory effect of eGFP. Most importantly, we found that secretion

20   of C1INH from fibroblasts carrying the c.551_685del allele was robustly increased,

21   although to a lesser extent than in control fibroblasts, after lentiviral *SERPING1* gene

22   delivery boosting the level of C1INH in the medium to 4,000 ng/mL (Figure 10B). Thus,

23   the dominant negative effects of the disease allele seemed to lower the total protein output

24   in patient cells, but did not severely restrict secretion of ectopically expressed C1INH

25   protein. These findings support the notion that conventional gene addition therapy

1   approaches can treat the disease and can be developed for future treatment also of HAE

2   type I involving dominant negative disease mechanisms.

Discussion

Since the initial description of HAE by Osler in 1888 (33) and later fundamental studies by Donaldson linking HAE with C1INH deficiency (34), the growing understanding of the disease pathophysiology of HAE has resulted in different HAE treatment modalities including intravenous C1INH concentrates and subcutaneous bradykinin receptor antagonists. However, cellular disease mechanisms responsible for the reduced levels of functional C1INH in the blood of HAE type I patients, compared to healthy individuals, are yet to be elucidated. A better understanding of the cellular pathology of HAE type I is essential to improve individualized treatment and pave the way for new effective treatments of the disease including genetic therapies. Based on earlier studies, it has been suggested that defective C1INH causes HAE type I through vaguely described 'trans-inhibitory' actions that may cause reduced functional C1INH plasma levels in HAE type I patients by negatively affecting synthesis, intracellular transport, or secretion of normal C1INH protein (29, 35). Speculations suggesting that C1INH variants that are defective in intracellular transport may negatively affect transport of normal C1INH were laid out 25 years ago (36). However, such trans-inhibitory mechanisms still remain to be unraveled.

In this study, we report that defective C1INH protein, at least for a subset of HAE type I patients, has the capacity to reduce the secretion of normal C1INH protein in a dominant negative fashion. Restricted secretion correlates with intracellular accumulation of both defective and normal C1INH protein in the ER and the formation of aggregates consisting of both C1INH variants linked by protein-protein interactions. We specifically studied skin-derived fibroblasts from a HAE type I patient carrying a dominant negative allele with a severe cellular phenotype and confirmed that C1INH protein retention

1   caused by aggregation was evident in patient cells. In this patient-derived cellular model

2   system, we also showed that increased levels of C1INH secretion could be achieved by

3   delivery of the wildtype *SERPING1* gene, demonstrating benefits of genetic restoration

4   despite the dominant negative effects of the disease gene. Additionally, we find that

5   secretion of normal C1INH from fibroblasts derived from healthy donors is restricted

6   when a dominant negative allele is transferred to the cells using a lentiviral delivery

7   approach.

8   Protein polymer formation is a characteristic of serpinopathies like A1ATD and

9   FENIB. In both cases, polymers of mutated serpins have been shown to accumulate

10   within the ER (19, 20, 22). Miranda and colleagues established a cellular model of FENIB

11   that reproduced aggregation of mutated neuroserpin polymers in the ER, as seen in the

12   patients, and found that the accumulation of neuroserpin within the ER was associated

13   with a structural change of the ER (37). Similarly, in our study, aggregates of C1INH

14   protein were found to accumulate within the ER in both HeLa cells co-transfected with

15   plasmids encoding normal and defective C1INH variants and in fibroblasts from a Danish

16   type I HAE patient carrying the c.551_685del *SERPING1* gene variant. Detection of

17   C1INH aggregates in the ER correlates with previous findings, in which mutant C1INH

18   was found to be sensitive to endoglycosidase H (endoH) (35, 36). Furthermore, the

19   accumulation within ER was reflected by structural change of ER, suggesting that C1INH

20   protein retention potentially affects ER function in C1INH-expressing cells in patients

21   and has wider impact on cellular homeostasis.

22   Biochemical analysis of neuroserpin polymers, isolated from the brain of a patient

23   with FENIB, revealed that neuroserpin polymers were composed of mutant neuroserpin

24   only (38). Along these lines, the polymerization rates of normal and defective α1-

25   antitrypsin are not affected by mixing of normal and defective protein (39), suggesting

1   that the disease-causing protein in A1ATD is not directly affecting the normal protein.

2   This is in accordance with the recessive inheritance of A1ATD. In contrast to these

3   findings, we found that 7 out of 16 analyzed HAE-causing C1INH variants (encoded by

4   SERPING1[c.551_685del],   SERPING1[c.550G>A],   SERPING1[c.566C>A],

5   SERPING1[c.530T>C], SERPING1[c.707T>C], SERPING1[c.863_864TC>AA], and

6   SERPING1[c.871A>C]) caused formation of aggregates containing normal C1INH.

7   Additionally, normal and defective C1INH protein was found to co-localize in such

8   aggregates, and Co-IP assays stated for all relevant C1INH variants that formation of

9   aggregates involves direct protein-protein interaction between normal and mutated

10   C1INH protein. Interestingly, except for cells expressing C1INH$_{Thr167Asn}$ (encoded by

11   SERPING1[c.566C>A]), we did not observe aggregate formation for any of the studied

12   C1INH variants, when the protein was expressed in the absence of normal C1INH. This

13   indicates that C1INH aggregates are prone to be formed when both functional and

14   defective C1INH proteins are present and involves unique lock-and-key interactions

15   between normal C1INH and disease-causing variants, providing further support to the

16   notion that defective C1INH reduces the secretion of normal C1INH by directly inducing

17   its retention. C1INH$_{Thr167Asn}$ encoded by SERPING1[c.566C>A] appeared to represent a

18   unique variant for which induced formation of polymers did not necessarily require

19   normal C1INH, although the mutant protein did indeed influence accumulation of co-

20   expressed normal C1INH. As the patient carrying this specific *SERPING1* variant showed

21   C1INH blood levels that were only slightly reduced relative to healthy individuals, one

22   may speculate that normal C1INH in this patient was to some degree left 'untouched' as

23   a result of the tendency of C1INH$_{Thr167Asn}$ to form homopolymers.

24   Throughout our studies, we observed the most severe cellular phenotypes

25   triggered by C1INH$_{Gly162\_Pro206del}$ derived from the c.551_685del *SERPING1* gene variant

1   due to the profound capacity of this variant to induce formation of C1INH aggregates in

2   the presence of normal C1INH protein. In Danish patients expressing this exon 4-deleted

3   mRNA, the disease allele contains a larger genomic deletion spanning exon 4 and

4   including parts of the flanking introns. Notably however, splice site mutations in this

5   region (typically in the splice acceptor site in the intron upstream of exon 4) can lead to

6   formation of the exact same mutated protein, and HAE type I patients with this particular

7   type of mutation have been described in previous reports (4, 40). Differences in the

8   potential to form C1INH aggregates among the different HAE-causing C1INH variants

9   and the particular severity of C1INH $_{Gly162\_Pro206del}$ may reflect how the mutation affects

10   the structure of the C1INH protein. The c.551_685 deletion in the *SERPING1* gene leads

11   to deletion of the whole exon 4, which induces significant structural changes in the

12   C1INH protein, as exon 4 encodes both hD (Helix D), hC (Helix C), and s2A. Both hD

13   and hC play an important role in stabilizing the shutter region (18), and deletion of these

14   two helices may lead to opening of the sA, thereby allowing the RCL of other C1INH

15   proteins to dock-in to the protein allowing stable protein-protein interactions. Opening of

16   the shutter domain may explain why aggregates are formed in cells co-expressing normal

17   C1INH and C1INH$_{Gly162\_Pro206del}$ or some of the other variants causing aggregation and

18   retention of C1INH. Interestingly, the c.530T>C, c.707T>C and c.863_863TC>AA

19   *SERPING1* gene variants (resulting in amino acid substitutions in hB, hE and s3A,

20   respectively, in C1INH protein), are all in very close proximity to the shutter domain and

21   the region which is deleted in C1INH $_{Gly162\_Pro206del}$ (including hD, hC, and s2A) (see

22   Supplementary Figure S12 for structural overview of the C1INH variations).

23   Furthermore, deletion of exon 4 or other variations in the part of the protein encoded by

24   this region may possibly lead to a less protruding RCL, potentially preventing it from

25   aggregating with itself. This could explain why aggregate formation is predominant in

1   the heterozygous situation where the mutant protein, like C1INH$_{Gly162\_Pro206del}$, is

2   expressed simultaneously with normal C1INH.

3   Our discoveries suggest that HAE type I can be classified as a true serpinopathy

4   with potential variations in cellular disease mechanisms depending on the specific

5   *SERPING1* gene variant. Differences in the level of aggregate formation induced by the

6   studied C1INH variants could potentially reflect that assays based on transient

7   transfection in some cases do not allow sufficient time for the build-up of aggregates.

8   Therefore, we cannot at this stage exclude that aggregate formation is part of the

9   pathogenesis also for C1INH variants that did not in our hands induce a distinct cellular

10   phenotype with formation of aggregates. Importantly, it cannot be ruled out that some of

11   these variants cause disease through other trans-inhibitory mechanisms or that

12   haploinsufficiency, potentially due to unbalanced gene expression from the two

13   *SERPING1* alleles, results in development of the disease. Common for the far majority

14   of the studied C1INH variants is that protein secretion, and not expression, is severely

15   affected by the mutation, and this may potentially in some patients trigger

16   haploinsufficiency even without the formation of aggregates. It should be noted that we

17   in our studies excluded *SERPING1* variants giving rise to severely truncated C1INH

18   variants or RNA degradation by nonsense-mediated decay. Therefore, disease-causing

19   mechanisms for these variants still need to be described. More studies including a larger

20   number of *SERPING1* variants will be essential to classify patients and their mutated gene

21   variant according to the cellular disease mechanisms, including the dominant negative

22   mechanisms that we have unveiled here.

23   Like C1INH, α1-antitrypsin is primarily produced in the liver. Polymerization and

24   intracellular retention of the mutated Z α1-antitrypsin variant within the ER of

25   hepatocytes causes juvenile hepatitis, cirrhosis and hepatocellular carcinoma (39). In our

1 cellular model system, we found that the exact same cellular phenotype with massive

2 aggregate formation appeared in cells expressing the Z α1-antitrypsin variant and in cells

3 co-expressing normal and defective C1INH. Inevitably, this could indicate that liver

4 damage observed in A1ATD patients could occur also in HAE type I patients. However,

5 to our knowledge, liver damage has not in general been reported in HAE type I patients,

6 indicating that such aggregate formation does not disturb normal liver function. Potential

7 differences in aggregate formation could be explained by different levels of expression

8 leading to differing intracellular concentrations of C1INH and A1AT, but potential

9 explanations are currently speculative. In addition, although we observed severe

10 aggregate formation in skin-derived fibroblasts, we did not have access to patient-derived

11 hepatocytes, and cannot exclude that this particular cellular phenotype is less pronounced

12 in the human liver. It is not unlikely that dominant negative retention of normal C1INH

13 may add to the consequences of haploinsufficiency complicating the interpretation of the

14 cellular pathology, but this will have to be addressed in future studies, potentially in

15 hepatocyte-like cells derived from patient-derived induced pluripotent stem cells (41, 42).

16 To the great benefit of patients, HAE type I is currently treated successfully with

17 intravenously administered C1INH concentrates. However, as clinical gene therapy

18 treatments of severe inherited conditions like blindness (43), primary immunodeficiency

19 (44), and hemophilia (45), are continuously showing great promise worldwide, it is not

20 unrealistic to envision future genetic treatments also of HAE. Recently, work by Qiu and

21 colleagues demonstrated reduced vascular leakage in skin and internal organs in a HAE

22 mouse model treated intravenously with adeno-associated virus (AAV)-based vectors

23 encoding functional C1INH (46). As HAE shares several similarities with hemophilia,

24 invaluable experience from ongoing hemophilia B trials based on AAV-based gene

25 delivery may eventually benefit HAE patients. Our discovery that HAE type I at least in

some patients involve dominant negative disease mechanisms would argue that these patients would not be suitable for conventional gene therapy based on *SERPING1* gene transfer. Nevertheless, our studies in patient cells suggest that the dominant-negative effects of the disease allele can be overcome by viral vector-based gene delivery facilitating solid C1INH expression after gene delivery. It remains unclear, however, whether compromised ER function may affect posttranslational modification and overall functionality of ectopically expressed C1INH. As transgenic HAE mouse models carrying dominant-negative disease alleles are not currently available, further experimental consolidation of the benefits of gene therapy awaits the development of a mouse model that mimics the genetics and disease of the patients. Also, such a model, for example carrying the *SERPING1* exon 4 deletion, will allow future studies aiming at describing and resolving C1INH protein aggregation in the liver of heterozygous carriers of the dominant-negative disease mutation.

1   **Methods**

2   Complete descriptions of methods and materials are provided in the Supplementary

3   Methods available on The Journal of Clinical Investigation web site.

Conflict of interest

No potential conflicts of interest were disclosed.

Author contributions

DH and JGM designed research studies. DH, LBR, IKR and KAS cloned the plasmids. DH, LBR, SSM, MKT, and ABB conducted experiments and acquired data. DH, LBR, SSM, ABB, LNN, and JGM analyzed data. IKR and AB isolated skin biopsies and analyzed patient data. LNN and TJC helped preparing and imaging cells. YP and CK produced antibodies. TF provided assistance to experiments carried out at the fluorescence scanner and co-immunoprecipation. LNN, TJC, TF, YP and CK provided reagents. DH and JGM wrote the manuscript.

References

1.   Bernstein JA. HAE update: epidemiology and burden of disease. *Allergy Asthma Proc.* 2013;34(1):3-6.

2.   Germenis AE, and Speletas M. Genetics of Hereditary Angioedema Revisited. *Clin Rev Allergy Immunol.* 2016;51(2):170-82.

3.   Bygum A. Hereditary angio-oedema in Denmark: a nationwide survey. *Br J Dermatol.* 2009;161(5):1153-8.

4.   Colobran R, Lois S, de la Cruz X, Pujol-Borrell R, Hernandez-Gonzalez M, and Guilarte M. Identification and characterization of a novel splice site mutation in the SERPING1 gene in a family with hereditary angioedema. *Clin Immunol.* 2014;150(2):143-8.

5.   Zuraw BL, and Christiansen SC. HAE Pathophysiology and Underlying Mechanisms. *Clin Rev Allergy Immunol.* 2016;51(2):216-29.

6.   Rosen FS, Pensky J, Donaldson V, and Charache P. Hereditary Angioneurotic Edema: Two Genetic Variants. *Science.* 1965;148(3672):957-8.

7.   Dewald G, and Bork K. Missense mutations in the coagulation factor XII (Hageman factor) gene in hereditary angioedema with normal C1 inhibitor. *Biochem Biophys Res Commun.* 2006;343(4):1286-9.

8.   Bork K, Wulff K, Steinmuller-Magin L, Braenne I, Staubach-Renz P, Witzke G, et al. Hereditary angioedema with a mutation in the plasminogen gene. *Allergy.* 2017.

9.   Bafunno V, Firinu D, D'Apolito M, Cordisco G, Loffredo S, Leccese A, et al. Mutation of the angiopoietin-1 gene (ANGPT1) associates with a new type of hereditary angioedema. *J Allergy Clin Immunol.* 2017.

10. Irving JA, Pike RN, Lesk AM, and Whisstock JC. Phylogeny of the serpin superfamily: implications of patterns of amino acid conservation for structure and function. *Genome Res.* 2000;10(12):1845-64.

11. Gettins PG. Serpin structure, mechanism, and function. *Chem Rev.* 2002;102(12):4751-804.

12. Heit C, Jackson BC, McAndrews M, Wright MW, Thompson DC, Silverman GA, et al. Update of the human and mouse SERPIN gene superfamily. *Hum Genomics.* 2013;7:22.

13. Law RH, Zhang Q, McGowan S, Buckle AM, Silverman GA, Wong W, et al. An overview of the serpin superfamily. *Genome Biol.* 2006;7(5):216.

14. Silverman GA, Bird PI, Carrell RW, Church FC, Coughlin PB, Gettins PG, et al. The serpins are an expanding superfamily of structurally similar but functionally diverse proteins. Evolution, mechanism of inhibition, novel functions, and a revised nomenclature. *J Biol Chem.* 2001;276(36):33293-6.

15. Schechter I, and Berger A. On the size of the active site in proteases. I. Papain. *Biochem Biophys Res Commun.* 1967;27(2):157-62.

16. Guo PC, Dong Z, Zhao P, Zhang Y, He H, Tan X, et al. Structural insights into the unique inhibitory mechanism of the silkworm protease inhibitor serpin18. *Sci Rep.* 2015;5:11863.

17. Huntington JA, Read RJ, and Carrell RW. Structure of a serpin-protease complex shows inhibition by deformation. *Nature.* 2000;407(6806):923-6.

18. Khan MS, Singh P, Azhar A, Naseem A, Rashid Q, Kabir MA, et al. Serpin Inhibition Mechanism: A Delicate Balance between Native Metastable State and Polymerization. *J Amino Acids.* 2011;2011:606797.

19. Lomas DA, Evans DL, Finch JT, and Carrell RW. The mechanism of Z alpha 1-antitrypsin accumulation in the liver. *Nature.* 1992;357(6379):605-7.

20. Davis RL, Shrimpton AE, Holohan PD, Bradshaw C, Feiglin D, Collins GH, et al. Familial dementia caused by polymerization of mutant neuroserpin. *Nature.* 1999;401(6751):376-9.

21. Tsutsui Y, Kuri B, Sengupta T, and Wintrode PL. The structural basis of serpin polymerization studied by hydrogen/deuterium exchange and mass spectrometry. *J Biol Chem.* 2008;283(45):30804-11.

22. Lomas DA, and Mahadeva R. Alpha1-antitrypsin polymerization and the serpinopathies: pathobiology and prospects for therapy. *J Clin Invest.* 2002;110(11):1585-90.

23. Madsen DE, Hansen S, Gram J, Bygum A, Drouet C, and Sidelmann JJ. Presence of C1-inhibitor polymers in a subset of patients suffering from hereditary angioedema. *PLoS One.* 2014;9(11):e112051.

24. Kaplan AP, and Ghebrehiwet B. The plasma bradykinin-forming pathways and its interrelationships with complement. *Mol Immunol.* 2010;47(13):2161-9.

25. Nussberger J, Cugno M, Amstutz C, Cicardi M, Pellacani A, and Agostoni A. Plasma bradykinin in angio-oedema. *Lancet.* 1998;351(9117):1693-7.

26. Wouters D, Wagenaar-Bos I, van Ham M, and Zeerleder S. C1 inhibitor: just a serine protease inhibitor? New and old considerations on therapeutic applications of C1 inhibitor. *Expert Opin Biol Ther.* 2008;8(8):1225-40.

27. Prada AE, Zahedi K, and Davis AE, 3rd. Regulation of C1 inhibitor synthesis. *Immunobiology.* 1998;199(2):377-88.

28. Cicardi M, Igarashi T, Rosen FS, and Davis AE, 3rd. Molecular basis for the deficiency of complement 1 inhibitor in type I hereditary angioneurotic edema. *J Clin Invest.* 1987;79(3):698-702.

29. Kramer J, Rosen FS, Colten HR, Rajczy K, and Strunk RC. Transinhibition of C1 inhibitor synthesis in type I hereditary angioneurotic edema. *J Clin Invest.* 1993;91(3):1258-62.

30. Basiji DA, Ortyn WE, Liang L, Venkatachalam V, and Morrissey P. Cellular image analysis and imaging by flow cytometry. *Clin Lab Med.* 2007;27(3):653-70, viii.

31. Kramer J, Katz Y, Rosen FS, Davis AE, 3rd, and Strunk RC. Synthesis of C1 inhibitor in fibroblasts from patients with type I and type II hereditary angioneurotic edema. *J Clin Invest.* 1991;87(5):1614-20.

32. Staunstrup NH, Madsen J, Primo MN, Li J, Liu Y, Kragh PM, et al. Development of transgenic cloned pig models of skin inflammation by DNA transposon-directed ectopic expression of human beta1 and alpha2 integrin. *PLoS One.* 2012;7(5):e36658.

33. Osler W. Landmark publication from The American Journal of the Medical Sciences: Hereditary angio-neurotic oedema. 1888. *Am J Med Sci.* 2010;339(2):175-8.

34. Donaldson VH, and Evans RR. A Biochemical Abnormality in Herediatry Angioneurotic Edema: Absence of Serum Inhibitor of C' 1-Esterase. *Am J Med.* 1963;35:37-44.

35. Ernst SC, Circolo A, Davis AE, 3rd, Gheesling-Mullis K, Fliesler M, and Strunk RC. Impaired production of both normal and mutant C1 inhibitor proteins in type

I hereditary angioedema with a duplication in exon 8. *J Immunol.* 1996;157(1):405-10.

36. Verpy E, Couture-Tosi E, Eldering E, Lopez-Trascasa M, Spath P, Meo T, et al. Crucial residues in the carboxy-terminal end of C1 inhibitor revealed by pathogenic mutants impaired in secretion or function. *J Clin Invest.* 1995;95(1):350-9.

37. Miranda E, Romisch K, and Lomas DA. Mutants of neuroserpin that cause dementia accumulate as polymers within the endoplasmic reticulum. *J Biol Chem.* 2004;279(27):28283-91.

38. Yazaki M, Liepnieks JJ, Murrell JR, Takao M, Guenther B, Piccardo P, et al. Biochemical characterization of a neuroserpin variant associated with hereditary dementia. *Am J Pathol.* 2001;158(1):227-33.

39. Mahadeva R, Chang WS, Dafforn TR, Oakley DJ, Foreman RC, Calvin J, et al. Heteropolymerization of S, I, and Z alpha1-antitrypsin and liver cirrhosis. *J Clin Invest.* 1999;103(7):999-1006.

40. Roche O, Blanch A, Duponchel C, Fontan G, Tosi M, and Lopez-Trascasa M. Hereditary angioedema: the mutation spectrum of SERPING1/C1NH in a large Spanish cohort. *Hum Mutat.* 2005;26(2):135-44.

41. Si-Tayeb K, Noto FK, Nagaoka M, Li J, Battle MA, Duris C, et al. Highly efficient generation of human hepatocyte-like cells from induced pluripotent stem cells. *Hepatology.* 2010;51(1):297-305.

42. Takayama K, Morisaki Y, Kuno S, Nagamoto Y, Harada K, Furukawa N, et al. Prediction of interindividual differences in hepatic functions and drug sensitivity by using human iPS-derived hepatocytes. *Proc Natl Acad Sci U S A.* 2014;111(47):16772-7.

43. Maguire AM, High KA, Auricchio A, Wright JF, Pierce EA, Testa F, et al. Age-dependent effects of RPE65 gene therapy for Leber's congenital amaurosis: a phase 1 dose-escalation trial. *Lancet.* 2009;374(9701):1597-605.

44. Hacein-Bey-Abina S, Hauer J, Lim A, Picard C, Wang GP, Berry CC, et al. Efficacy of gene therapy for X-linked severe combined immunodeficiency. *N Engl J Med.* 2010;363(4):355-64.

45. Nathwani AC, Tuddenham EG, Rangarajan S, Rosales C, McIntosh J, Linch DC, et al. Adenovirus-associated virus vector-mediated gene transfer in hemophilia B. *N Engl J Med.* 2011;365(25):2357-65.

46. Qiu T, Chiuchiolo MJ, Whaley AS, Russo AR, Sondhi D, Kaminsky SM, et al. Gene Therapy for C1 Esterase Inhibitor Deficiency in a Murine Model of Hereditary Angioedema. *Allergy.* 2018.

Figures
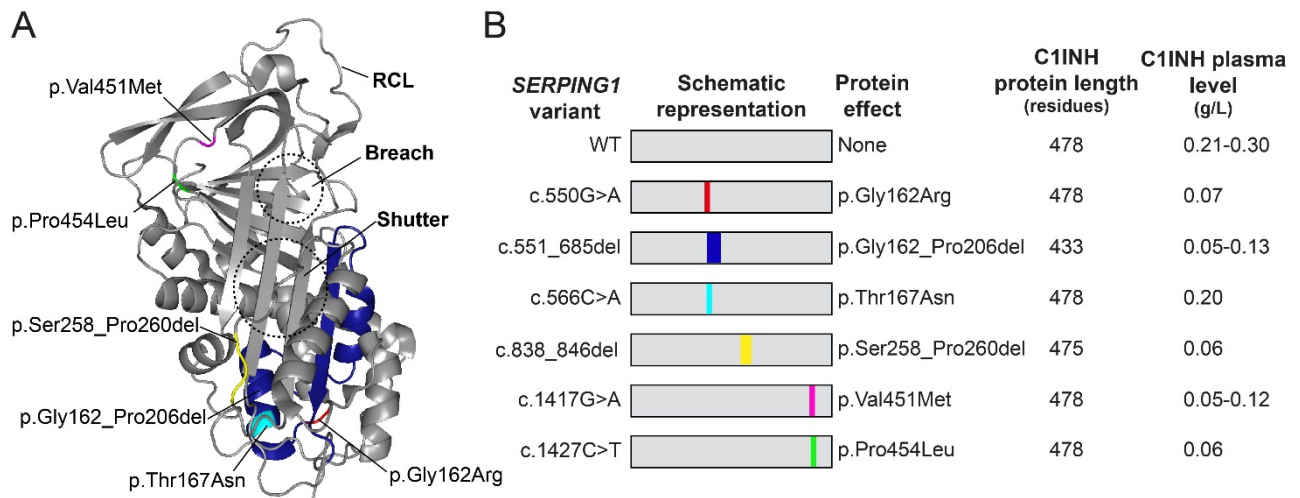
Figure 1. Characteristics of studied *SERPING1* gene variants and plasma levels of C1INH in patients carrying the variants (A) The overall structure of active C1INH protein (PDB entry 5DU3). The locations of the studied HAE causing variants are marked as follow: p.Gly162Arg (red), p.Thr167Asn (cyan), p.Val451Met (magenta) and p.Pro454Leu (green). For p.Gly162_Pro206del and p.Ser258_Pro260del the area deleted in C1INH is marked with dark blue and yellow, respectively. **(B)** Presentation of the six studied *SERPING1* gene variants and key data related to each gene variation and to patients carrying the variants. See Supplementary Table S1 for additional information.
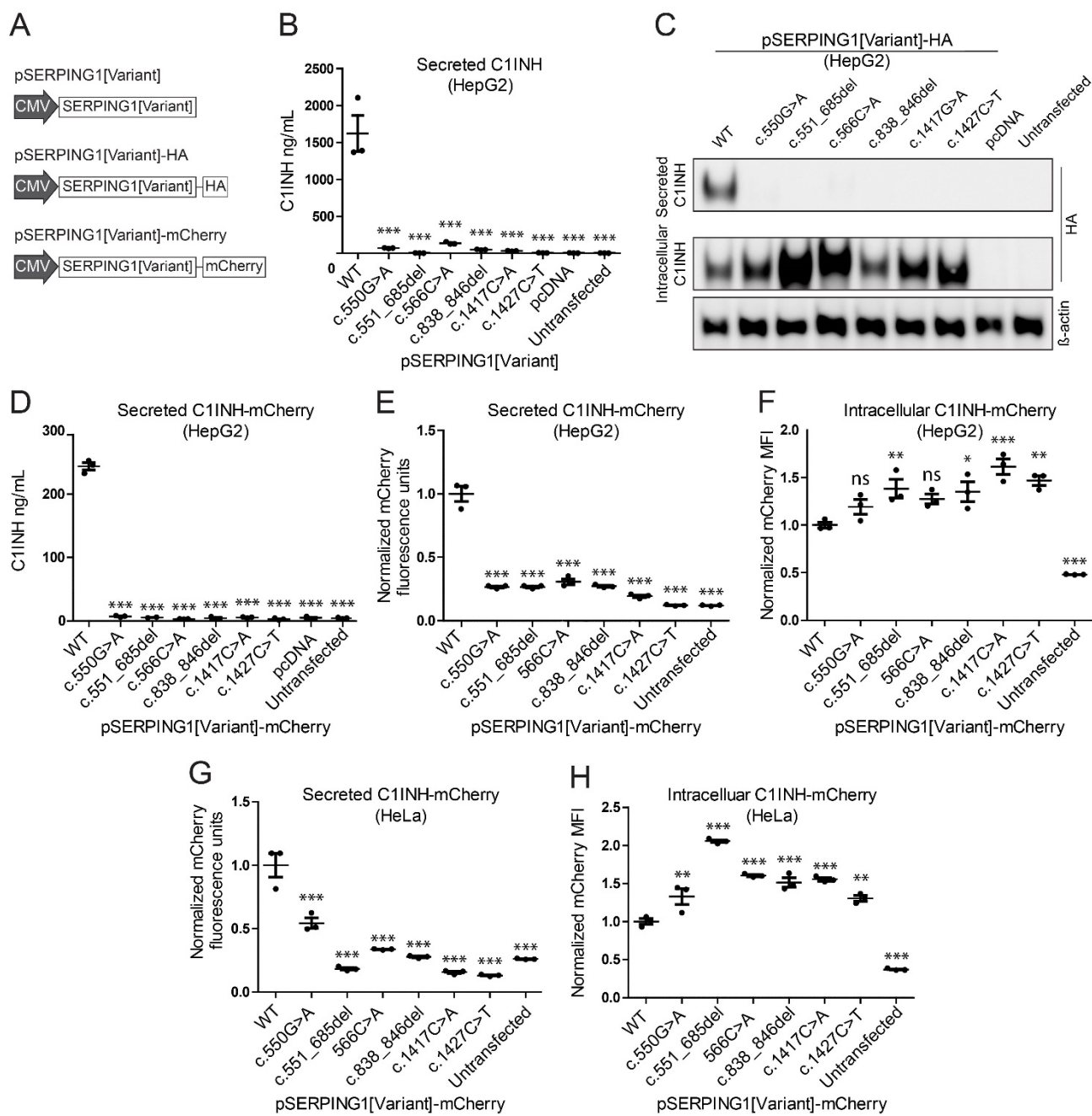
Figure 2. Expression and severely reduced secretion of C1INH encoded by the six studied *SERPING1* gene variants. (A) Schematic representation of the vector types used in this study to express *SERPING1* gene variants. Black arrows indicate the promoter derived from cytomegalovirus (CMV). **(B)** C1INH levels in medium from HepG2 cells transfected with 900 ng pSERPING1[Variant] measured by ELISA. **(C)** Western blot analysis of medium protein and total protein derived from HepG2 cells transfected with

900 ng pSERPING1[Variant]-HA. The secreted and intracellular C1INH levels were detected using a HA-specific antibody. **(D)** C1INH levels in medium from HepG2 cells transfected with 900 ng pSERPING1[Variant]-mCherry measured by ELISA. **(E, F)** Secreted and intracellular levels of C1INH in HepG2 cells measured by mCherry fluorescence intensity. **(G, H)** Secreted and intracellular levels of C1INH in HeLa cells measured by mCherry fluorescence intensity. Cells were transfected with different pSERPING1[Variant]-mCherry vectors. The amount of C1INH-mCherry secreted into the medium was determined using a fluorescence scanner **(E, G)** and the intracellular level by flow cytometry **(F, H)**. **(B-H)** Transfections were carried out in triplicates ($n = 3$), and similar results were seen in at least two independent experiments. Data are depicted as mean $\pm$ SEM. * $P < 0.05$, **$P < 0.01$, ***$P < 0.001$, compared with WT. Statistical analyses were performed by 1-way ANOVA with Dunnett's multiple comparison test. MFI, Median Fluorescence Intensity.
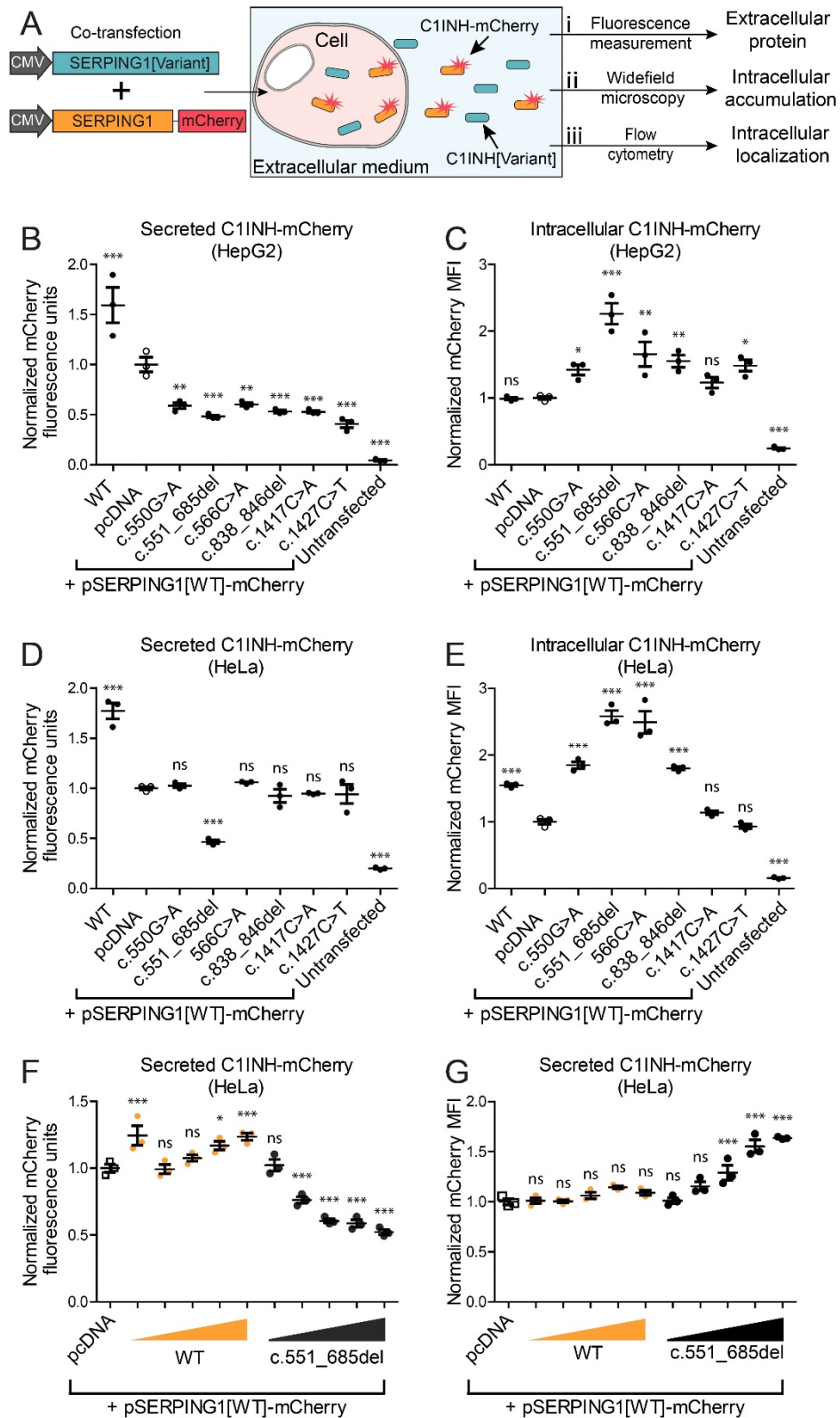
Figure 3. Negative impact of C1INH encoded by HAE-causing *SERPING1* gene variants on secretion of normal C1INH-mCherry correlates with increased intracellular protein levels. (A) Schematic representation of the cellular assay system.

Cells were co-transfected with pSERPING1[Variant] and pSERPING1[WT]-mCherry. Expression of mCherry-fused normal C1INH allowed evaluation of the effect of different *SERPING1* gene variants on (i) secretion (ii) intracellular retention, and (iii) intracellular localization of normal C1INH-mCherry. **(B, C)** Levels of secreted and intracellular C1INH-mCherry in HepG2 cells co-transfected with 450 ng of both pSERPING1[Variant] and pSERPING1[WT]-mCherry. **(D, E)** Levels of secreted and intracellular C1INH-mCherry in HeLa cells transfected as in (B, C). Secretion of normal C1INH-mCherry was measured by fluorescence scanning **(B, D)** and the intracellular level by flow cytometry **(C, E). (F)** Increasingly restricted C1INH secretion with higher levels of mutant C1INH. Dose-response experiment was carried out in HeLa cells. Cells were co-transfected with 450 ng pSERPING1[WT]-mCherry and 50, 200, 450, 700 or 900 ng of pSERPING1[WT] or pSERPING1[c.551_685del]. pcDNA plasmid was included in all transfections to ensure a total amount of 1350 ng plasmid DNA in each transfection reaction. **(G)** Intracellular levels of C1INH-mCherry in cells described in (F). **(B-G**) Transfections were carried out in triplicates (*n* = 3), and similar results were seen in at least three independent experiments. Data are depicted as mean $\pm$ SEM. * P < 0.05, **P < 0.01, ***P < 0.001, compared with pcDNA. Statistical analyses were performed by 1-way ANOVA with Dunnett's multiple comparison test. MFI, Median Fluorescence Intensity.
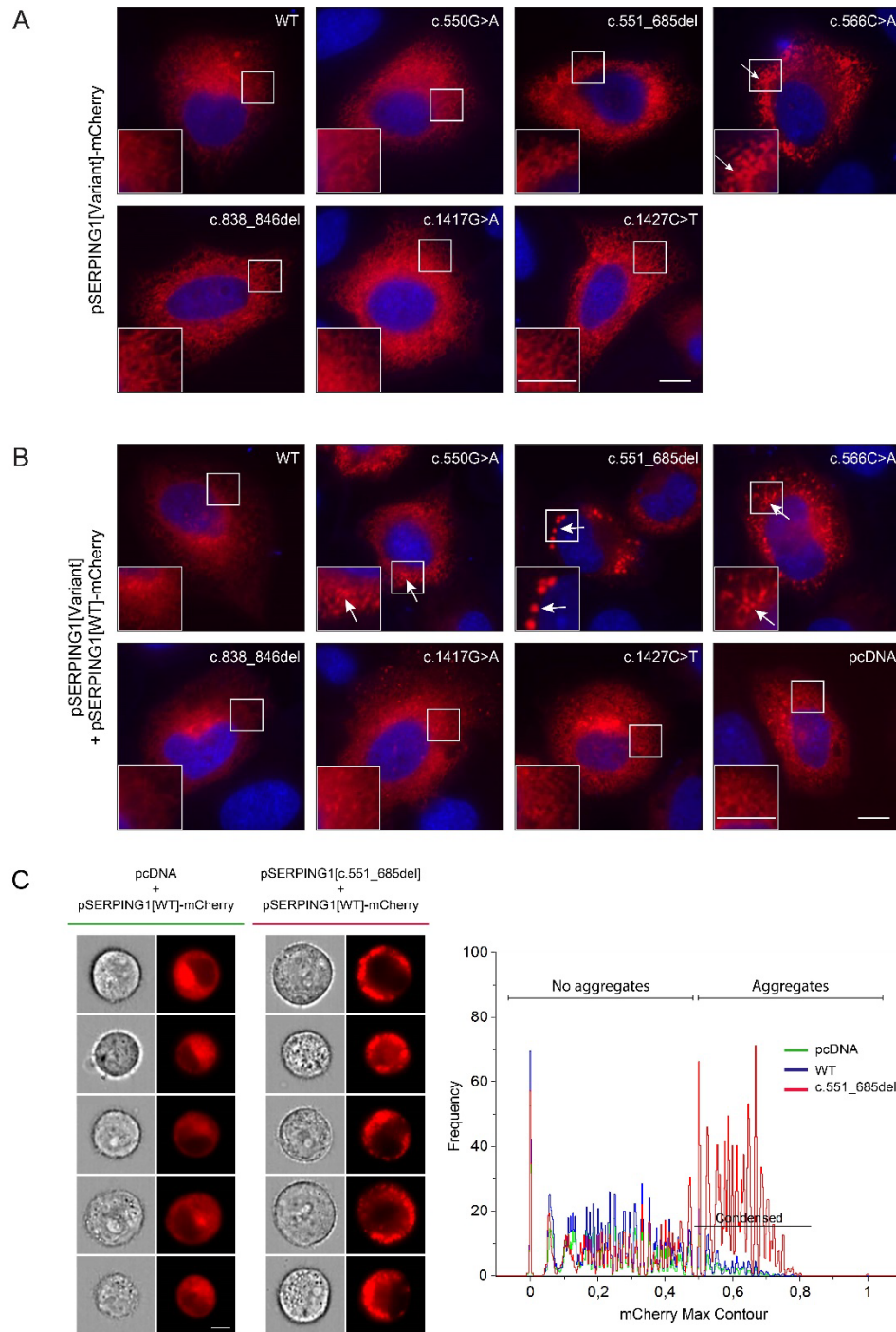
Figure 4. Intracellular localization of C1INH-mCherry detected by widefield microscopy and Imagestream® analysis. **(A)** Intracellular localization of normal and mutated C1INH-mCherry (red). Live widefield microscopy of HeLa cells cultured for 48 hours after transfection with 900 ng pSERPING1[Variant]-mCherry. **(B)** Intracellular

localization of normal C1INH-mCherry (red) in the presence of HAE-causing *SERPING1* gene variants. Live widefield microscopy of HeLa cells cultured for 48 hours after co-transfection with 450ng pSERPING1[WT]-mCherry (red) and 450ng pSERPING1[Variant] gene variants. Aggregates of normal C1INH-mCherry were detectable in cells co-transfected with pSERPING1[WT]-mCherry and vectors encoding the following *SERPING1* variants: c.550G>A, c.551_685del or c.566C>A. Examples of aggregates are indicated with white arrows. Cells were incubated with Hoechst to visualize nuclei (blue). **(C)** High prevalence of C1INH aggregates in cells expressing normal and c.551_685del *SERPING1* gene variants. HeLa cells were co-transfected with pSERPING1[WT]-mCherry and either pcDNA, pSERPING1[WT] or pSERPING1[c.551_685del]. The cells were analyzed by Imaging Flowcytometry using Imagestream® technology, and cells with C1INH aggregates were identified to have a max contour above 0.5 (condensed). Two sets of columns (left panels) show light/fluorescence microscopy images of cells expressing SERPING1[WT]-mCherry in the presence of pcDNA and pSERPING1[c.551_685del], respectively. Scale bar: 7 μm. Right panel: Imagestream-based quantification of larger cell populations, showing aggregate formation predominantly in cells co-transfected with pSERPING1[WT]-mCherry and pSERPING1[c.551_685del] (red graph). Number (*n*) of condensed cells relative to the number of mCherry-positive cells were as follows: pSERPING1[WT]-mCherry + pcDNA, *n*=262/2137; pSERPING1[WT]-mCherry + pSERPING1[WT], *n*=159/1395; pSERPING1[WT]-mCherry + pSERPING1[c.551_685del], *n*=2115/3579. **(A-B)** Scale bars: 10 μm. Data are representative of findings from more than three biological replicates, and similar results were seen in at least three independent experiments.
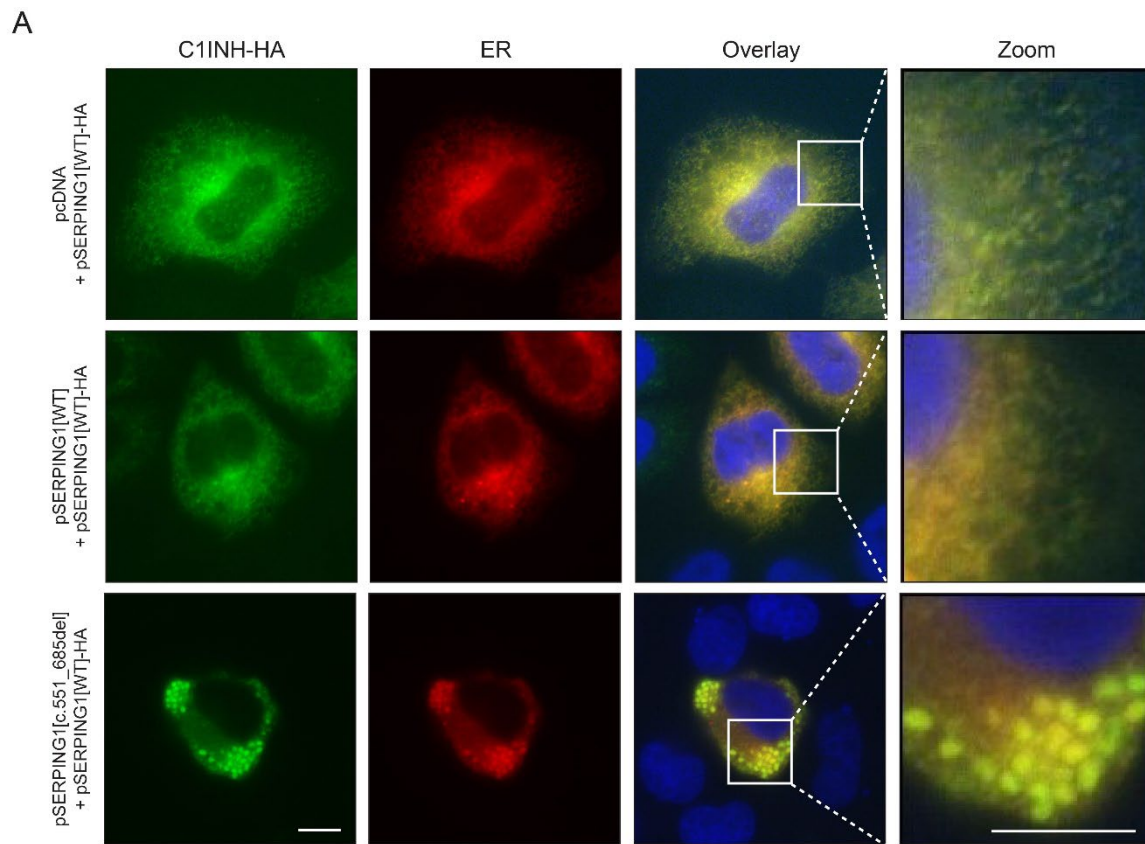
Figure 5. Intracellular retention of C1INH and α1-antitrypsin in the ER. HeLa cells were co-transfected with pSERPING1[WT]-HA and pcDNA, pSERPING1[WT] or pSERPING1[c.551_685del]. To visualize ER an expression plasmid encoding the Tomato fluorescence gene fused to an endoplasmic reticulum targeting sequence was included in the transfections (red). 48 hours after the co-transfections the cells were fixated and incubated with a HA-antibody and Hoechst to visualize normal C1INH-HA (green) and the nuclei (blue), respectively. Scale bars: 10 μm. Data are representative of findings from more than three biological replicates, and similar results were seen in at least three independent experiments.
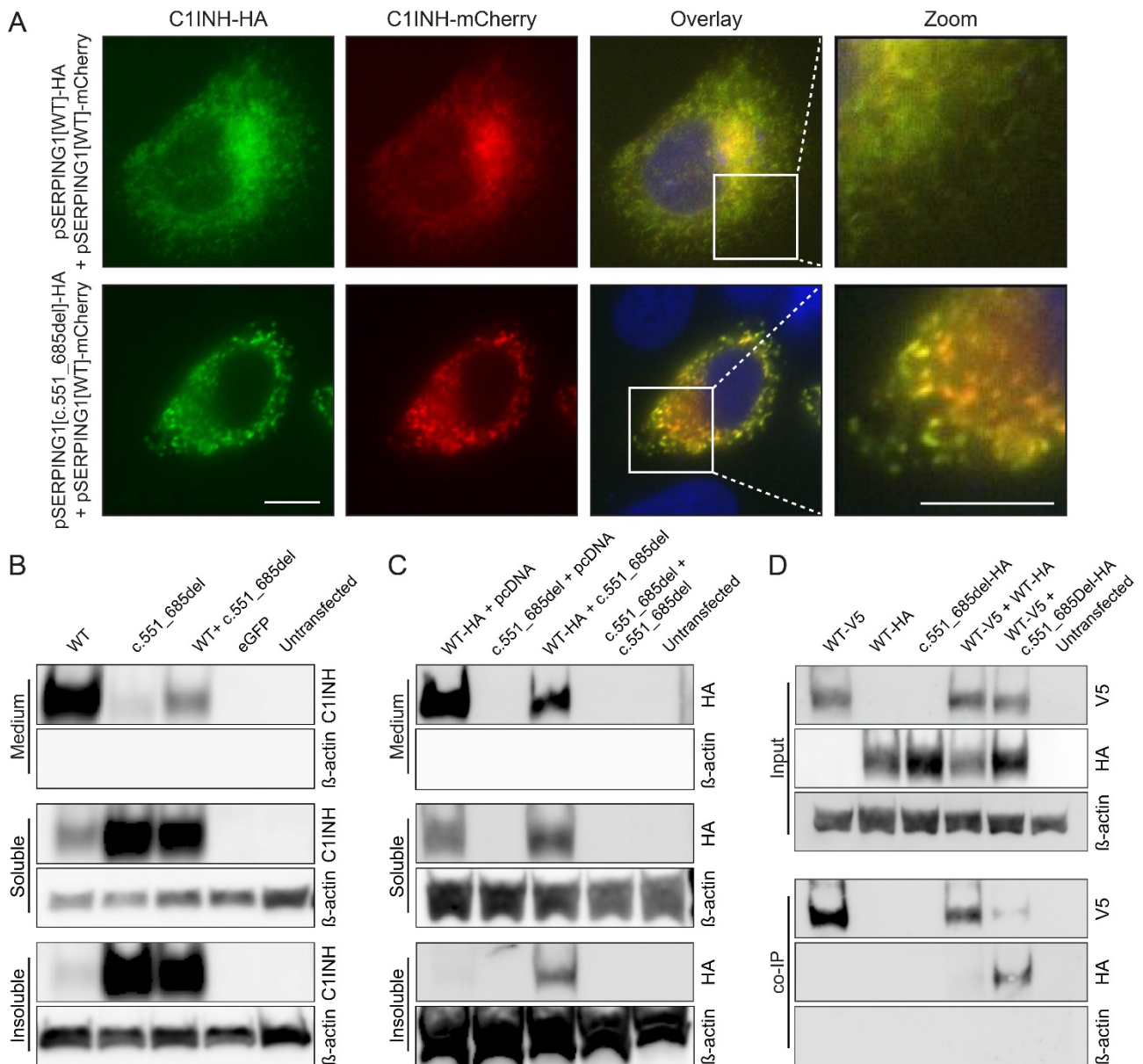
Figure 6. Direct interaction between normal C1INH and C1INH$_{Gly162\_Pro206del}$. (A)
Co-localization of normal and mutated C1INH. Widefield microscopy of HeLa cells
cultured for 48 hours after co-transfection with SERPING1[WT]-mCherry and
SERPING1[WT]-HA or SERPING1[c.551_685del]-HA. C1INH-HA was visualized
with HA-specific antibody (Green) and nuclei with Hoechst (blue). Scale bars: 10 μm.
(B-C) Western blot analysis of total protein in medium as well as soluble and insoluble

protein fractions derived from HeLa cells cultured for 72 hours after transfection or co-transfection with 900 ng plasmid DNA in total. Separation of soluble and insoluble C1INH fractions by centrifugation of whole cell lysate at 12000g for 20 minutes at 4°C. **(B)** Detection of C1INH$_{Gly162\_Pro206del}$ in the insoluble fraction. HeLa cells were transfected with 900 ng pSERPING1[WT] or pSERPING1[c.551_685del] or co-transfected with 450 ng pSERPING1[WT] and 450 ng pSERPING1[c.551_685de]. C1INH levels were detected using PAb C1INH antibody. **(C)** Normal C1INH in the insoluble fraction induced by C1INH$_{Gly162\_Pro206del}$. HeLa cells were co-transfected with 450 ng pSERPING1[WT]-HA and either 450 ng pcDNA or pSERPING1[c.551_685del]. Normal C1INH-HA levels were detected with HA-specific antibody. **(D)** Direct protein-protein interaction between normal and mutated C1INH. Co-immunoprecipitation on whole cell lysate from HeLa cells cultured for 48 hours after transfection or co-transfection with 40 µg plasmid DNA in total. HeLa cells were transfected with pSERPING1[WT]-V5, pSERPING1[WT]-HA or pSERPING1[c.551_685del]-HA, or co-transfected with pSERPING1[WT]-V5 and pSERPING1[WT]-HA or pSERPING1[c.551_685del]-HA. A small amount of the whole cell lysate was saved (input) and the remaining lysate incubated with anti-V5 coupled beads to capture normal V5-tagged C1INH and interacting proteins (co-IP). Presence of normal C1INH-V5 and C1INH[Variant]-HA was visualized with V5- and HA-specific antibodies as relevant. **(A)** Data are representative of findings from more than three biological replicates. **(A-C)** Similar results were seen in at least two independent experiments. **(B-D)** Transfections were carried out in triplicates (n = 3).
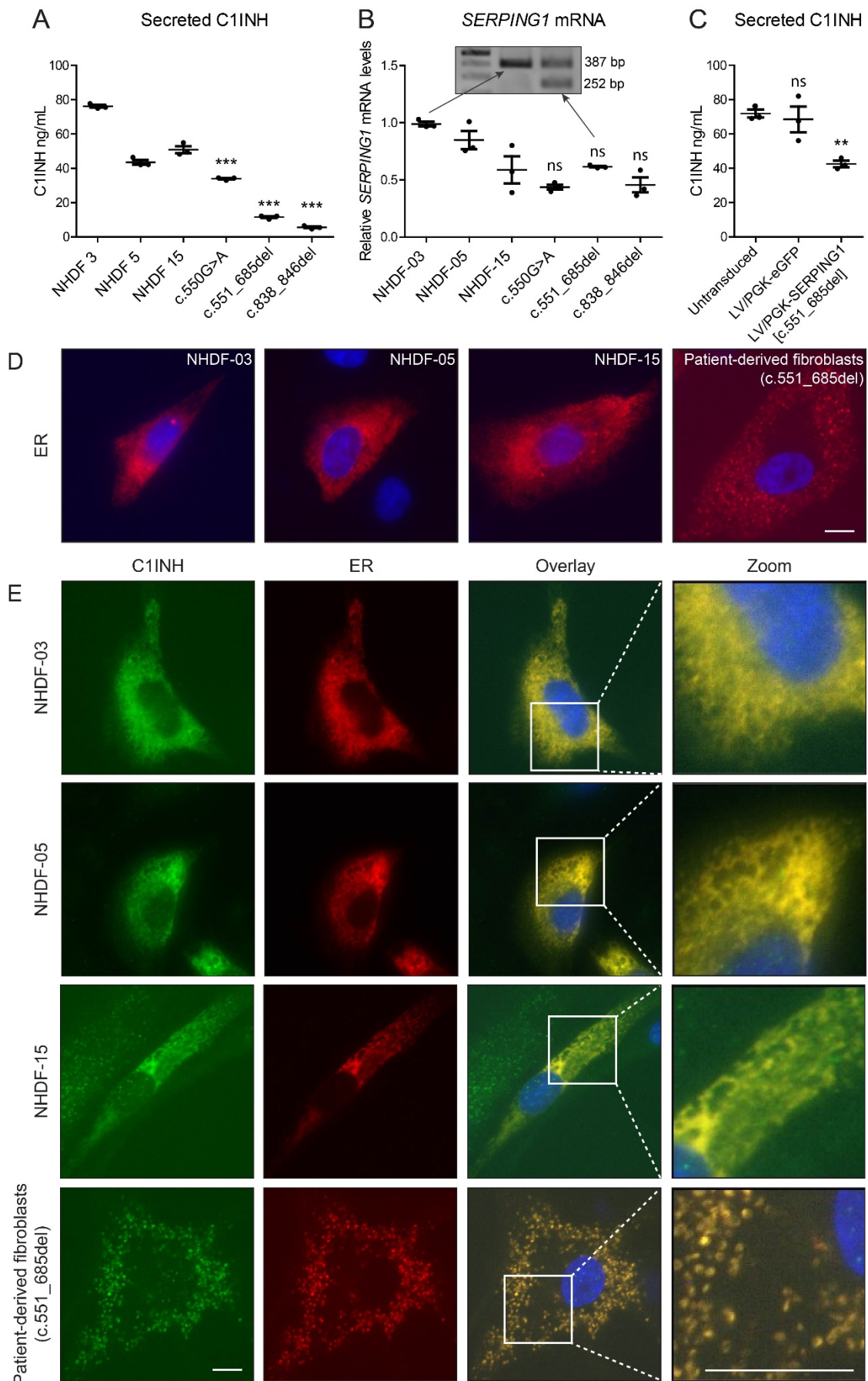
Figure 7. Correlation of reduced C1INH secretion in skin-derived fibroblasts derived from a patient carrying the c.551_685del mutation with C1INH

accumulation in ER. (A) C1INH in medium from control (NHDF-03, NHDF-05, NHDF-15) and patient-derived fibroblasts. **(B)** Evaluation of *SERPING1* mRNA expression levels in control and patient-derived fibroblasts by qPCR. Equal expression of normal and mutant *SERPING1* alleles in fibroblasts derived from the patient carrying the c.551_685del mutation. Insert: Agarose gel showing PCR products from PCR amplification (using primers spanning the deletion) on cDNA synthesized from RNA purified from either control NHDF-03 fibroblasts or patient-derived fibroblasts. **(C)** Restricted C1INH secretion induced by lentiviral delivery of *SERPING1*[c.551_685del]. Control NHDF-03 fibroblasts were transduced with lentiviral vectors encoding C1INH $_{Gly162\_Pro206del}$ (or eGFP as control) at an estimated MOI of 1. **(D)** Structure of the ER in control fibroblasts and fibroblasts derived from the c.551_685del patient. The fibroblasts were transfected with 900 ng of plasmid encoding the Tomato fluorescence gene fused to an ER-targeting sequence to visualize ER (red). Cells were fixated 48 hours after transfections, and nuclei visualized with Hoechst (blue). **(E)** Accumulation of endogenous C1INH within the ER of patient-derived fibroblasts. The fibroblasts were transfected as in (D), fixated, and incubated with Hoechst to visualize the nuclei (blue) and C1INH antibody to visualize both normal and mutated C1INH (green). **(A-C)** The experiment was carried out in triplicates ($n = 3$), and data are depicted as mean $\pm$ SEM. * $P < 0.05$, **$P < 0.01$, ***$P < 0.001$, patient-derived fibroblasts compared with NHDF-05 (A) or NHDF-15 (B) or transduced compared with untransduced NHDF-03 (C). Statistical analyses were performed by 1-way ANOVA with Dunnett's multiple comparison test. **(D-E)** Scale bars: 10 μm. Data are representative of findings from more than three biological replicates. **(A-E)** Similar results were seen in at least two independent experiments.
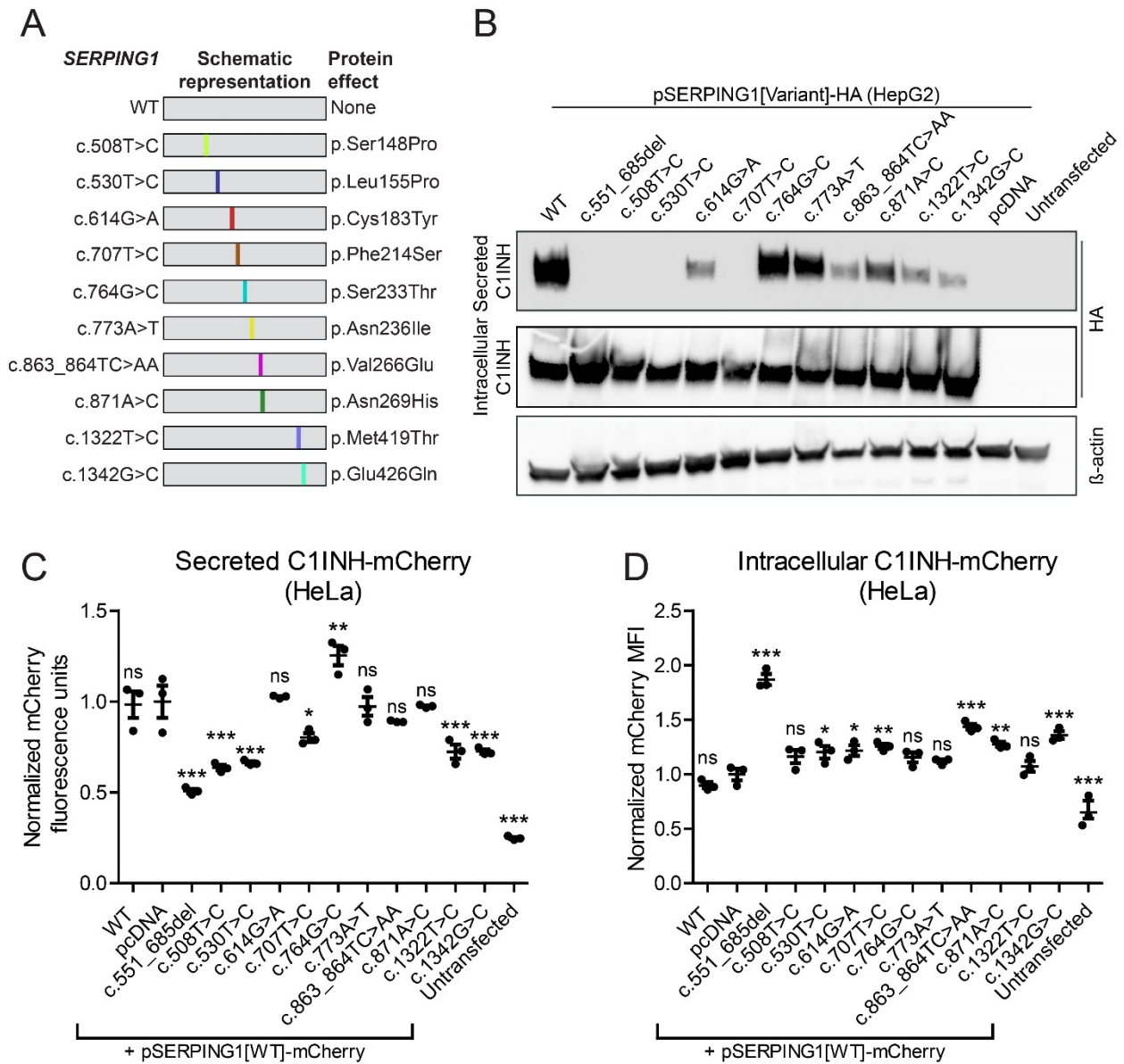
Figure 8. Dominant negative properties of additional HAE-causing *SERPING1* gene variants. (A) Schematic representation of studied *SERPING1* gene variants. See Supplementary table S2 for additional information. **(B)** Western blot analysis of medium and total protein derived from HepG2 cells transfected with 900 ng pSERPING1[Variant]-HA. The C1INH-HA levels were detected using a HA-specific antibody. **(C-D)** Secretion and intracellular levels of normal C1INH-mCherry in HeLa cells co-transfected with 450 ng pSERPING1[WT]-mCherry and 450 ng

pSERPING1[Variant]. **(B-D)** Transfections were carried out in triplicates (n=3), and similar results were seen in at least two independent experiments. **(C-D)** * P < 0.05, **P < 0.01, ***P < 0.001, compared with pcDNA. Statistical analyses were performed by 1-way ANOVA with Dunnett's multiple comparison test.
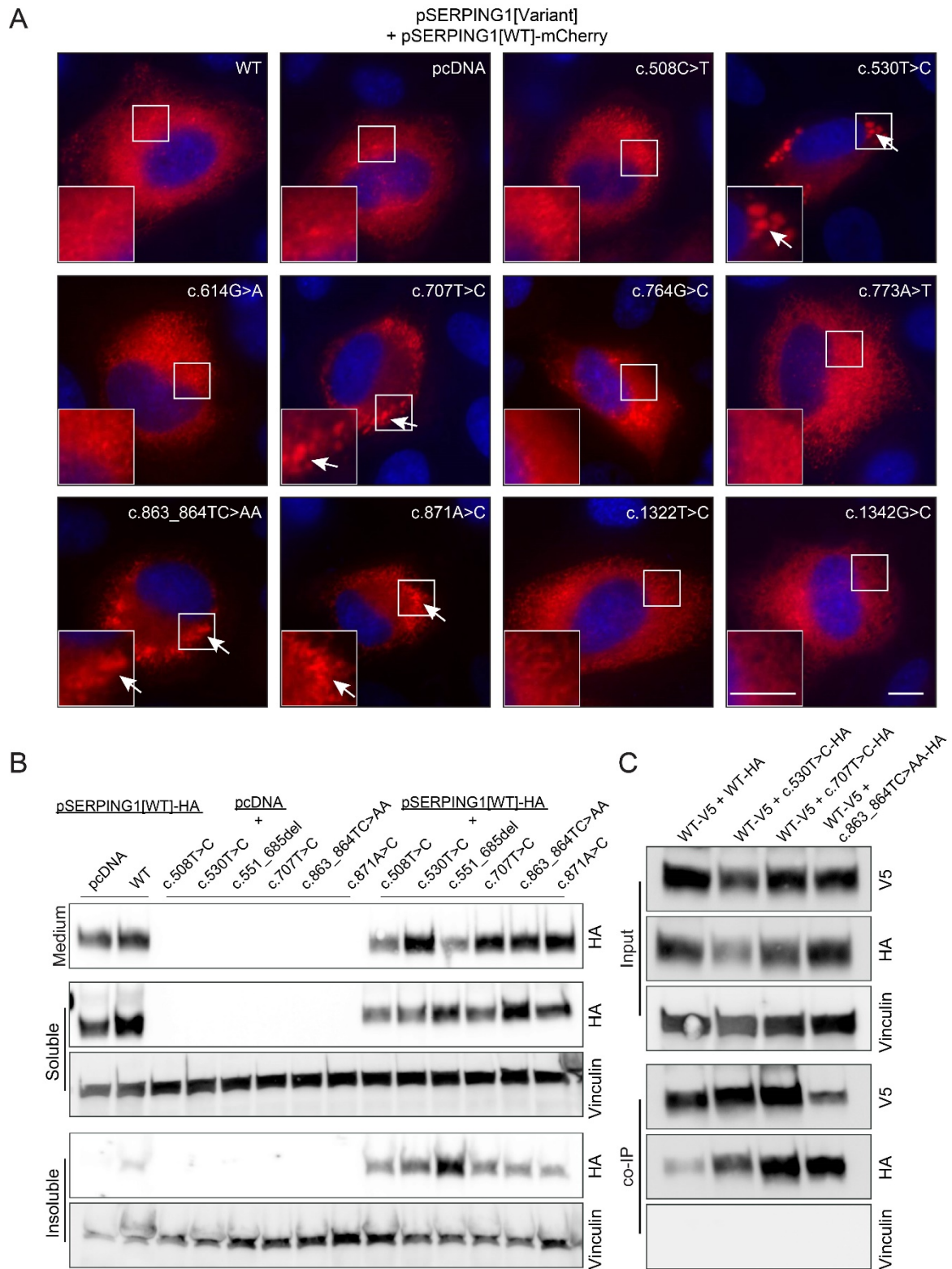
Figure 9. Formation of C1INH aggregates containing associated normal and mutant C1INH induced by dominant negative *SERPING1* gene variants causing HAE. (A) Live widefield microscopy of HeLa cells cultured for 48 hours after co-transfection with 450ng pSERPING1[WT]-mCherry and 450 ng pSERPING1[Variant]. Aggregates are

indicated with arrows. Scale bars: 10 µm. **(B)** Western blot analysis of medium, soluble and insoluble C1INH derived from HeLa cells cultured for 72 hours after co-transfection with 450 ng pSERPING1[WT]-HA and 450 ng pSERPING1[Variant]. The experiment was carried out as described in Figure 6B-C. **(C)** Co-immunoprecipitation on cell lysate from HeLa cells cultured for 48 hours after co-transfection with 20 µg pSERPING1[WT]-V5 and 20 µg pSERPING1[Variant]-HA. The experiment was carried out as described in Figure 6D. **(A-B)** Data are representative of findings from more than three biological replicates and similar results were seen in at least two independent experiments. Transfections were carried out in triplicates (n=3) **(B)** or duplicates ($n = 2$) **(C)**.
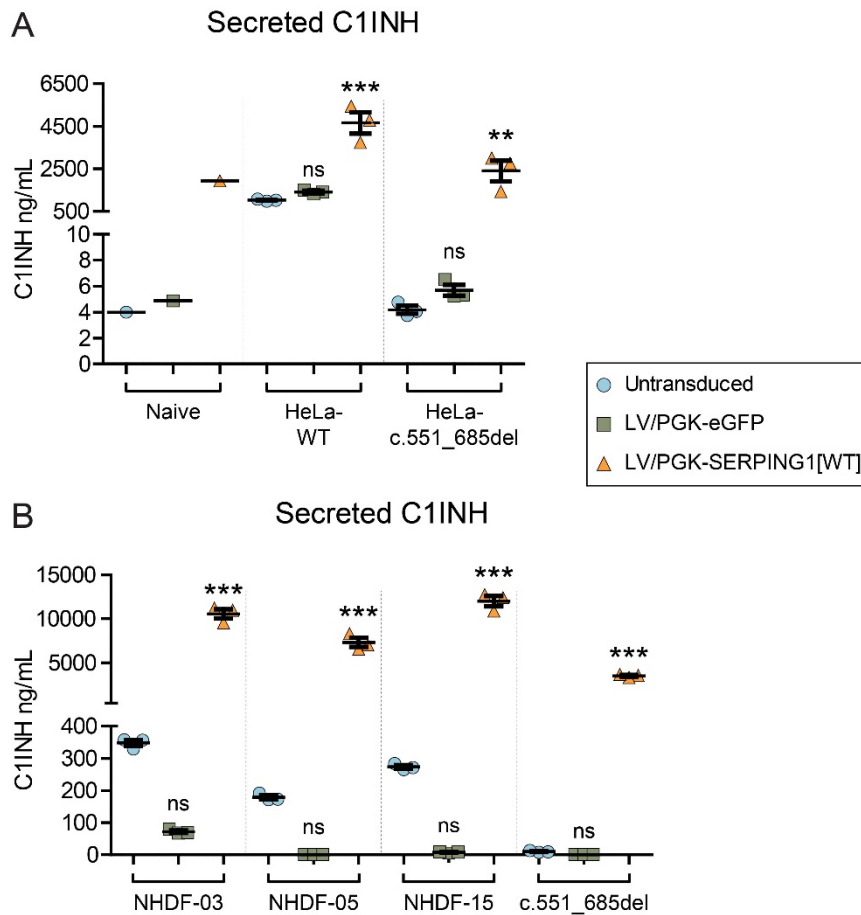
Figure 10. Increased C1INH secretion after lentiviral delivery of wildtype *SERPING1* gene models HAE gene therapy in fibroblasts from patients carrying a dominant-negative disease allele (*SERPING1*[c.551_685del]). (A) HeLa-WT and HeLa-c.551_685del cell populations (3 of each) were created by transduction of naïve HeLa cells with lentiviral vectors encoding normal C1INH or C1INH$_{Gly162\_Pro206del}$. Stably transduced and naïve HeLa cells were reseeded and transduced with lentiviral vectors encoding eGFP or normal C1INH. Transduction of each of the three cell populations was carried out in triplicates (n=3), and the medium was pooled for each transduced cell population prior to C1INH measurements. For the naïve cell line, cells were transduced and medium pooled prior to C1INH measurement, resulting in only a single data point

for each treatment. **(B)** Control and patient-derived fibroblasts were transduced with lentiviral vectors encoding normal C1INH or eGFP as a control. Transductions were carried out in triplicates (*n*=3). **(A-B)** Data are depicted as mean + SEM. * P < 0.05, **P < 0.01, ***P < 0.001, compared with untransduced cells in each group. 'ns' refers to lack of statistical significance between untransduced and LV/PGK-eGFP-treated groups. Statistical analyses were performed by 1-way ANOVA with Dunnett's multiple comparison test. **(B)** Similar results were seen in at least two independent experiments. LV, lentiviral vectors.